SOLUTION OF ONE-DIMENSIONAL TRANSIENT FLOW IN FRACTURED AQUIFERS BY NUMERICAL LAPLACE TRANSFORM INVERSION

A THESIS SUBMITTED TO
THE GRADUATE SCHOOL OF NATURAL AND APPLIED SCIENCES
OF
MIDDLE EAST TECHNICAL UNIVERSITY

BY

SERDAR DÜNDAR

IN PARTIAL FULFILLMENT OF THE REQUIREMENTS

FOR

THE DEGREE OF MASTER OF SCIENCE

IN

CIVIL ENGINEERING

NOVEMBER 2005

Approval of the Graduate School of Natural and Applied Sciences

_____

Prof. Dr. Canan ÖZGEN

Director

I certify that this thesis satisfies all the requirements as a thesis for the degree of Master of Science.

_____

Prof. Dr. Erdal ÇOKÇA

Head of Department

This is to certify that we have read this thesis and that in our opinion it is fully adequate, in scope and quality, as a thesis for the degree of Master of Science.

_____

Prof. Dr. Halil ÖNDER

Supervisor

Examining Committee Members

Prof. Dr. Halil Önder   (METU,CE) ————————

Assoc. Prof. Dr. Nuray Tokyay   (METU,CE) ————————

Assoc. Prof. Dr. Ismail Aydın   (METU,CE) ————————

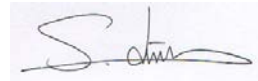Asst. Prof. Dr. Burcu Altan Sakarya (METU,CE) ————————

Dr. Yakup Darama   (D.S.İ) ————————

I hereby declare that all information in this document has been obtained and presented in accordance with academic rules and ethical conduct. I also declare that, as required by these rules and conduct, I have fully cited and referenced all material and results that are not original to this work.

Name, Last Name: SERDAR DÜNDAR

Signature:

ABSTRACT

SOLUTION OF ONE-DIMENSIONAL TRANSIENT FLOW IN FRACTURED AQUIFERS BY NUMERICAL LAPLACE TRANSFORM INVERSION

DÜNDAR, Serdar

M.Sc., Department of Civil Engineering

Supervisor: Prof. Dr. Halil Önder

November 2005, 71 pages

Laplace transform step-response functions are presented for one dimensional transient flow in fractured semi-infinite & finite aquifers. Unsteady flow in the aquifer resulting from a constant discharge pumped from the stream is considered. Flow is one-dimensional, perpendicular to the stream in the confined aquifers. The stream is assumed to penetrate the full thickness of the aquifer. The aquifers may be semi-infinite or finite in width. The Laplace domain solutions are numerically inverted to the real-time domain with the Stehfest (1970) algorithm. During the course of the thesis a simple computer code is written to handle the algorithm and the code is verified by applying it to the one-dimensional transient flow in

a semi-infinite homogeneous aquifer problem which can be solved analytically to crosscheck with the numerical results.

Keywords: Transient Flow, Double Porosity Model, Stehfest Algorithm, Laplace Transform, Groundwater Flow, Numerical Modeling.

ÖZ

ÇATLAKLI AKİFERLERDE TEK BOYUTLU ZAMANA BAĞIMLI AKIMIN SAYISAL LAPLACE GERİ DÖNÜŞÜM YÖNTEMİYLE ÇÖZÜMÜ

Dündar, Serdar

Yüksek Lisans, İnşaat Mühendisliği Bölümü

Tez Yöneticisi: Prof. Dr. Halil Önder

Kasım 2005, 71 sayfa

Bu çalışmada sınırlı ve yarı sınırsız akiferlerdeki tek boyutlu süreksiz akım için Laplace transformasyonuyla elde edilmiş akifer tepki fonksiyonları elde edilmiştir. Nehirden sabit basınçlı pompaj yapılması durumunda akiferde meydana gelen değişken akım incelenmiştir. Akım tek boyutlu, basınçlı akiferde nehire dik gerçekleşmektedir.Nehirin akifer kalınlığı boyunca sürekli olduğu varsayılmıştır. Akifer genişliği yarı-sonsuz veya sonlu olabilir. Laplas düzleminde elde edilen sonuçlar daha sonra nümerik bir geri dönüşüm tekniği olan Stehfest (1970) algoritması kullanılarak reel düzleme aktarılmıştır. Bu algoritmanın kolaylıkla

uygulanabilmesi için kısa bir bilgisayar kodu çalısma sırasında yazılmıştır. Ve bu kod literatürde çözümleri analitik olarak bilinen yeraltı problemlerine –yarı sınırlı homojen akiferdeki akım ve tek boyutlu süreksiz akım- uygulanarak sonuçlarının doğruluğu kanıtlanmıştır.

Anahtar Kelimeler: Süreksiz Akım, Çift Geçirgenlik Modeli, Laplas Transformasyonu, Zamana Bağlı Yeraltı Suyu Akımı, Sayısal modelleme.

To my family

ACKNOWLEDGMENTS

I offer my sincere appreciation to my supervisor Prof. Dr. Halil Önder for his endless thoughtfulness and wise supervision throughout the research.

Special thanks go to my colleagues Günes Göler, Cüneyt Taşkan, Can Ersen Fırat, Kerem Önal, Özgür Kocak, Bora Yeşiltepe for their indispensable companionship and morale support.

I would like to thank to my manager Philip Wright, my colleague John Woodward and the chairman of Roger Bullivant Ltd., Roger Bullivant for their great support during my first year in UK.

Chris Downey, The Director of SCS Europe, deserves my special thanks for his support during the course of this study.

Finally, I express very special thanks to my family for their patience and unshakable faith in me, and for being with me whenever and wherever I needed their support.

TABLE OF CONTENTS

LIST OF FIGURES

LIST OF TABLES

LIST OF SYMBOLS

h_0	:	Initial Piezometric head averaged over the thickness of the aquifer, [L]
h_1	:	Piezometric head in the fractures averaged over the thickness of the aquifer, [L]
h_2	:	Piezometric head in the blocks averaged over the thickness of the aquifer, [L]
L	:	Length of the aquifer, [L]
N	:	Number of terms to sum in the Stehfest series, [-]
p	:	Laplace transform parameter, [-]
Q	:	Constant discharge rate (base flow) of the drain $(L^3 T^{-1})$
Q_b	:	Constant discharge rate (base flow) of the drain per unit length of drain $(L^2 T^{-1})$
Q_d	:	Dimensionless discharge (-)
S	:	Coefficient of Storage, [-]
S_1	:	Coefficient of Storage of the fractures, [-]
S_2	:	Coefficient of Storage of the blocks, [-]
T	:	Coefficient of transmissivity [$L^2 T^{-1}$]
T_1	:	Coefficient of transmissivity of the fractures, [$L^2 T^{-1}$]
T_2	:	Coefficient of transmissivity of the blocks, [$L^2 T^{-1}$]
t	:	Time, [T]
x	:	Distance along the flow direction, [L]

y	:	Dimensionless distance along x direction, [-]
z_1	:	Dimensionless drawdown in the fractures, [-]
z_2	:	Dimensionless drawdown in the blocks, [-]
ε	:	Shape factor relating to the geometry of the fractured rock, [L^{-2}]
δ	:	Dimensionless constant, (Eq. 4.10)
η	:	Dimensionless constant, (Eq. 4.10)
θ	:	Dimensionless time, [-]
v	:	Hydraulic diffusivity, [LT^{-1}]

CHAPTER 1

INTRODUCTION

Increased demand for water associated with population growth has heightened public awareness of the importance of the proper management of limited water resources. With this awareness, water-resource managers have taken considerable interest in quantification of the interaction of surface water and ground water. Analytical models are helpful tools in this endeavor.

One perceived difficulty in the use of analytical models is the fact that the necessary boundary conditions —stream stage and regional recharge or evapotranspiration— change continuously. While it is recognized that the effects of variable boundary conditions can be simulated with numerical models, the literature is full with analytical solutions for the interaction of confined, leaky, and water-table aquifers with an adjoining stream. A detailed but not fully comprehensive review of these solutions and their applications is provided by Moench and Barlow (2000) and will not be repeated here.

The groundwater flow behavior in an aquifer between a stream and an impervious boundary under natural or artificial conditions has to be known in various engineering applications. The prediction of the drawdown distribution in the aquifer and the prediction of the discharge from the stream in evaluation, in slope stability problems when a reservoir with variable water level is built on the stream are some

examples. The flow behaviour in a finite aquifer system due to a sudden rise or decline of the water level in the adjacent stream has been studied by many investigators (Rorabaugh, 1960; Rorabaugh, 1964; Pinder et al. 1969; Venetis, 1970; Önder 1994). In those studies, aquifers consisting of granular media were considered. However, a widely encountered type of aquifer, which can be found quite often around the world as a water-bearing formation, is fractured rock. These formations are known as a heterogeneous medium in which the blocks having very low permeability and containing the great amount of storage are separated by the fractures of high permeability. It is usually assumed that the conducting properties of the aquifer are associated with the fracture permeability, while the storage properties are related to the primary porosity of the blocks. (Barenblatt, et al.,1960 Huyakorn and Pinder, 1983).

Double porosity model is first introduced by Barenblatt et al. (1960) as a conceptual model to study the flow in fractured formations. This approach has been followed closely by other investigators. In such studies an exchange of water between fractures and blocks has been taken into account. In one group of studies it has been assumed that the flow from fractures to blocks takes place under pseudo-steady state conditions (Barenblatt et al., 1960; Warren&Root, 1963).Streltsova (1988) called this approach a lumped parameter model. In another group it has been assumed that the flow occurs under fully transient conditions (Kazemi, 1969; Kazemi et al., 1969) and Streltsova(1976) analyzed the radial flow case. Bear et al. (1993) recently gave a comprehensive treatment of flow and contamination transport in fractured rocks. According to Moench (1984), well test data obtained in the field support the assumption of the pseudo-steady state fracture-to-block flow assumption. However, on theoretical grounds alone, it is difficult to justify use of this assumption. Introducing the concept of a fracture skin, Moench (1984) showed that pseudo-state state fracture-

to-block flow is a special case of transient fracture-to-block flow with a fracture skin. The assumption of pseudo-steady state fracture-to-block flow has the advantage over the transient flow assumption of providing the greater mathematical simplicity; hence this assumption is used in this study (Önder, 1998).

In this study, numerically inverted Laplace transform solutions are presented for semi-infinite and finite fractured aquifers. The Laplace domain solutions are numerically inverted to the real-time domain with the Stehfest (1970) algorithm (more detail may be found in Moench and Ogata, 1982).

1.1   Mathematical Background

In general, specifying the flow domain might be a trivial or a major question in formulating the ground-water flow problem. The governing equation is the ground-water flow equation (Hsieh, 2002), expressed as;

$$\frac{\partial}{\partial x}(K_x \frac{\partial h}{\partial x}) + \frac{\partial}{\partial y}(K_y \frac{\partial h}{\partial y}) + \frac{\partial}{\partial z}(K_z \frac{\partial h}{\partial z}) = S_s \frac{\partial h}{\partial t} \qquad (1.1)$$

Where;

K_x, K_y, K_z are hydraulic conductivity in three directions

h is the hydraulic head

S_s is the specific storage

t is time

x,y,z are the distances in coordinate directions

Eq. 1.1 is derived from the combination of the continuity equation and the Darcy's Law.

If the porous medium is assumed to be homogeneous K and Ss become constant in space.

Different approaches are utilized to solve the groundwater problems as explained in the most general way above. Because of the nature and complexity of the groundwater problems; many analytical solutions are available, but not all of them can readily be evaluated numerically or sometimes even the analytical solution may not be obtained. The independent "time" variable makes the equations even more difficult to deal with. This is where the Laplace transform is introduced to make the equation independent from the time variable so that it is easier to be solved. The result of this solution will be in Laplace domain, and need to be inverted to obtain the solution in the real domain. The inversion method chosen is Stehfest algorithm which is a numerical inversion method easily applied with a subroutine written during course of this study.

1.2   Statement of the Problem

Double porosity models are used to describe flow in a medium composed of two components with distinctly different hydraulic properties. It is often applied to fractured porous rocks—the two components being the fractures and the porous intact rock (matrix). The fracture system is characterized by high hydraulic conductivity and low specific storage, while the matrix system is characterized by low hydraulic conductivity and high specific storage. In effect, the fractures provide the pathways for flow, while the matrix provides the source of water to a well (Hsieh, 2002).

Another example of an aquifer that might be represented as a double porosity medium is one composed of sand with clay lenses. The sand would play the role of the fractures, while the clay lenses would play the role of the matrix (Hsieh, 2002).

4

In this study, one dimensional flow in a confined fractured aquifer is analyzed using the double porosity approach assuming pseudo-steady state fracture-to-block flow under a prescribed flux condition at the stream boundary rather than under a step drawdown condition in the stream. The width of the aquifer is either semi-infinite or finite. It is believed that the outcome will be of use in the determination of storage and yield characteristics and of the recharge capability of strip shape fractured aquifers. The method utilized through the study consists of solving the differential equations in the Laplace domain for semi-infinite and finite fractured aquifers which are then numerically inverted to the real-time domain with the Stehfest (1970) algorithm (Moench and Ogata, 1982). Following Hall and Moench (1972), the stream is assumed to penetrate the full thickness of the aquifer as shown in the following figure
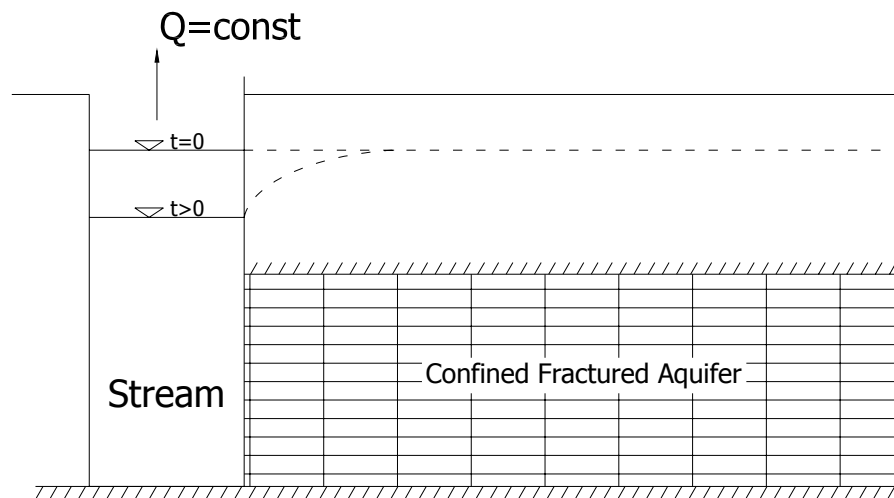
Figure 1.1: Drawdown in a confined fractured aquifer under a constant discharge

1.3 Objective of the study

The objective of this study is to demonstrate the advantage of working in Laplace plane. The Stehfest algorithm of the Laplace transform inversion is applied to several problems like the ones above –

which don't have a readily available analytical solution in the literature-and to the ones whose analytical solutions are available already, in order to prove the validity of the subroutines and for comparison of the results.

1.4   Description of the Thesis :

In the first chapter the statement of the problem and introductory comments are presented together with the objective of the work.

Chapter 2 provides a definitive and informative overview for the river-fractured aquifer interaction containing the mathematical background of the methods utilized during the study.

Chapter 3 involves the proof of the methods utilized. Several common groundwater problems are solved with Laplace transform and Stehfest algorithm procedure and the results are compared against the analytical solutions which are readily available. The problems solved in this chapter are involved with groundwater flow in homogeneous aquifers whose results are used in the later chapters to compare against the fractured aquifer cases.

Chapter 4 involves the application of the numerical methods to the chosen groundwater problems which do not have analytical solutions in the literature at the moment. These problems are involved in fractured aquifers.

Chapter 5 covers the evaluation, interpretation, and comparison of the results of the numerical study. Ferris' equations are used as the basis of the comparisons in this chapter.

Summary, discussions and conclusions together with recommendations are presented in Chapter 6.

CHAPTER 2

MATHEMATICAL FORMULATION OF RIVER – FRACTURED AQUIFER INTERACTION PROBLEM

2.1   Introduction

The fracture system is characterized by high hydraulic conductivity and low specific storage, while the matrix system is characterized by low hydraulic conductivity and high specific storage. In effect, the fractures provide the pathways for flow, while the matrix provides the source of water to fractures (Önder, 1998).

In the application of the double porosity conceptual model, a naturally fractured medium is separated into two overlapping continua, each filling the entire domain (Figure 2.1). The flow takes place both through pores of blocks and through fractures. The fluid is transferred between fractures and blocks, but there is no flow between any blocks. At each geometric point of a fractured medium, following the continuum concept, two sets of medium and flow parameters and variables are introduced, the first set being for the fracture flow and the second being for the flow in the blocks (Önder, 1998).

For the model to adequately represent a real aquifer, it is necessary for the fractures be closely spaced relative to the scale of the problem (for example, the distance between wells). In other words, the "representative elementary volume (REV)" should contain a large number of fractures and matrix blocks, so the inclusion or deletion of a

few fractures and matrix blocks would not substantially alter the hydraulic properties of the REV. The representative elementary volume at the geometric point under consideration consists of a sufficient number of porous blocks as well as a sufficient number of fractures having random distribution, orientation and size.
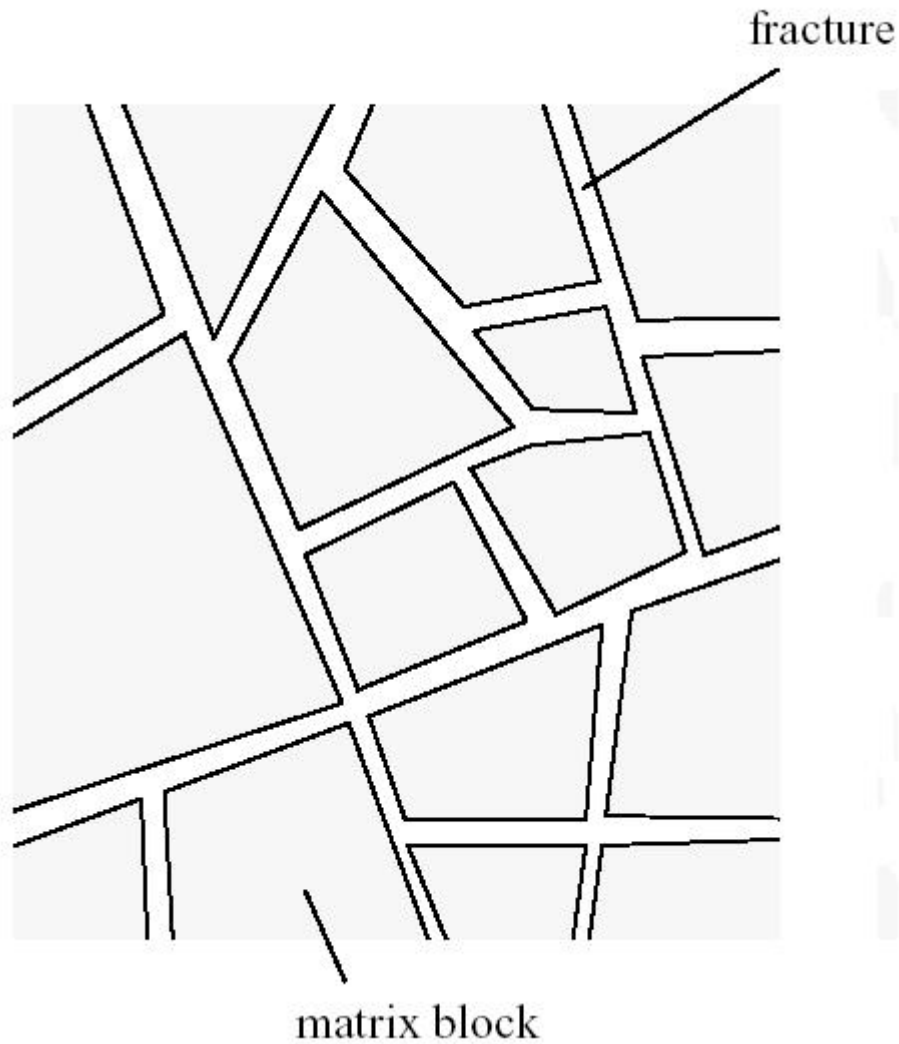
Figure 2.1: Representation of a system of fractures and matrix blocks [Bolton and Streltsova (1977)].

2.2   Mathematical Statement of the Problem

A complete statement of a ground-water flow problem requires specifying: (a) the extent of the flow domain, (b) the governing differential equation, (c) spatial distribution of properties, for example, hydraulic conductivity and specific storage, (d) boundary conditions, and (e) initial condition (for transient problems).The flow equations can be written separately for the fractures and for the matrix.

For the flow region, two cases, namely semi-infinite and finite aquifers, will be considered.

2.2.1 Governing Differential Equations

The one dimensional confined fracture flow may be obtained by combining the continuity equation and Darcy's Law, which leads to; (Önder, 1998):

$$T_1 \frac{\partial^2 h_1}{\partial x^2} = S_1 \frac{\partial h_1}{\partial t} + S_2 \frac{\partial h_2}{\partial t} \qquad (2.1)$$

In a similar way, the differential equation governing flow in the blocks is (Önder, 1998):

$$S_2 \frac{\partial h_2}{\partial t} = \varepsilon T_2 (h_1 - h_2) \qquad (2.2)$$

where;

T_i is the coefficient of transmissivity (i=1,2)

S_i is the coefficient of storage (i=1,2)

h_i is the mean piezometric head averaged over the thickness of the aquifer (i=1,2)

x is the distance along the flow direction

t is the time

ε relates to the geometry of the fractured rock. It may be viewed as a shape factor and has the dimension of inverse area

Subscript 1 denotes fracture flow whereas subscript 2 denotes the flow in blocks
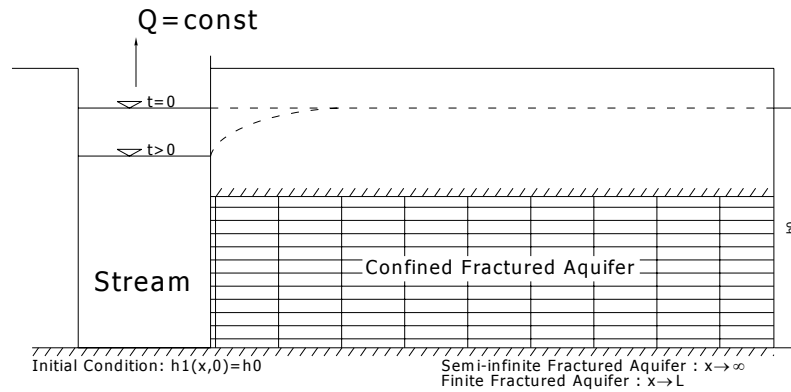
Figure 2.2: One dimensional transient flow

2.2.2 Initial and Boundary Conditions

The initial and boundary conditions to be satisfied by h_1 and h_2 for the problems considered in this work may be written as follows;

Case 1. One dimensional transient flow in a semi-infinite fractured aquifer:

Initial conditions:

$$h_1 = h_0 \text{ at t=0} \tag{2.3}$$

$$h_2 = h_0 \text{ at t=0} \tag{2.4}$$

Boundary conditions:

$$\lim_{x \to 0} \frac{\partial h_1}{\partial x} = -\frac{Q}{T_1} \tag{2.5}$$

$$\lim_{x \to \infty} h_1 = h_0 \qquad\qquad (2.6)$$

where;

Q is the volumetric discharge rate

Case.2   One dimensional transient flow in a finite fractured aquifer:

Initial conditions

$$h_1 = h_0 \text{ at t=0} \qquad\qquad (2.7)$$

$$h_2 = h_0 \text{ at t=0} \qquad\qquad (2.8)$$

Boundary conditions:

$$\lim_{x \to 0} \frac{\partial h_1}{\partial x} = -\frac{Q}{T_1} \qquad\qquad (2.9)$$

$$\lim_{x \to L} \frac{\partial h_1}{\partial x} = 0 \qquad\qquad (2.10)$$

2.2.3 Assumptions

This section describes the simplifying assumptions used in the above formulation. The following assumptions apply to both problems in this study:

1. Darcy's Law is valid for the flows both in fractures and blocks

2. Fractures and blocks are homogeneous and isotropic

3. The aquifer is confined and non-leaky, and its thickness is constant

4. Flow occurs only in x direction

5. The geometry of fractures is unaffected by chemical dissolution or deposition

6. Flow is fully saturated.

11

7. The lower and upper boundaries of each aquifer are horizontal and impermeable.

8. Hydraulic properties of the aquifers do not change with time.

9. The porous medium and fluid are slightly compressible.

10. The water level in the stream is initially at the same elevation as the water level everywhere in the aquifer

11. The stream forms a vertical boundary to the aquifer and fully penetrates the aquifer.

12. The stream flows in a straight line (that is, without sinuoisity).

(Önder 1998; Moench & Barlow, 2000)

2.3   Analytical Solution

One perceived difficulty in the use of analytical models is the fact that the necessary boundary conditions –stream stage and regional recharge or evapotranspiration- change continuously. During the course of this study one of the most widely used analytical methods, Laplace transform, is combined with a numerical inversion method, the Stehfest algorithm, to solve complex groundwater problems.

2.3.1 Laplace Transform

The Laplace transform is a powerful method for solving partial differential equations. Typically, the Laplace transform removes the time derivative term, so that we only have to deal with the spatial derivative terms. The Laplace transform of a function $u(t)$ is obtained by multiplying $u(t)$ by e^{-pt} and integrating the result with respect to t from t=0 to t=∞. By this procedure, we obtain a new function, called the Laplace transform of $u(t)$ and denoted by $\bar{u}(p)$, which is a function of p, the Laplace transform parameter. In other words;

$$\bar{u}(p) = \int_0^\infty u(t).e^{-pt}dt \qquad (2.11)$$

The Laplace transform parameter p can be thought of as an inverse time. In other words, large p corresponds to small time, and small p corresponds to large time.

The elementary properties of Laplace transform can be found from various Calculus literature. Some of the very basic properties which are used in this study are given below (Hsieh, 2002):

1. The Laplace transform is a linear transform. In other words, the Laplace transform of $u(t)+v(t)$ is $\bar{u}(p)+\bar{v}(p)$, and the Laplace transform of $Au(t)$ is $A\bar{u}(p)$, where A is a constant.

2. The Laplace transform of a constant A is A/p.

3. The Laplace transform of the derivative $\dfrac{du}{dt}$ is $p\bar{u}(p)-u(0)$.

4. If u is a function of t and additional independent variables, for example, $u = u(t,x)$, then the Laplace transform of $\dfrac{\partial^n u}{\partial x^n}$ is $\dfrac{\partial^n \bar{u}}{\partial x^n}$.

2.3.2 Stehfest Algorithm – Numerical Inversion of Laplace Transform

Inversion of the Laplace transform may be accomplished by: a) use of tables, if $\bar{u}(p)$ is a simple function, b) complex integration, or c) numerical inversion. For groundwater applications, tables are not always adequate. Complex integration is often possible but requires very complicated evaluations. Numerical inversion, is simple and often effective, and will serve as main tool in the course of this study.

Of the many numerical algorithms for Laplace inversion, the Stehfest (1970) algorithm is utilized in this study. If $\bar{u}(x,p)$ is the Laplace transform, then the inverse (that is, the original function) $u(x,t)$ can be approximately calculated by

$$u(x,t) \approx (\frac{\ln(2)}{t})\sum_{i=1}^{N} V_i \bar{u}(x,i\frac{\ln(2)}{t}) \qquad (2.12)$$

In the above equation the quantity $i\dfrac{\ln(2)}{t}$ substitutes for the Laplace parameter p. In this expression i is summation variable and t is time. The coefficients V_i are given by;

$$V_i = (-1)^{(N/2)+i} \sum_{k=(i+1)/2}^{\min(i,N/2)} \frac{k^{N/2}(2k)!}{(N/2-k)!k!(k-1)!(i-k)!(2k-1)!} \quad (2.13)$$

where *N* is an even number and *k* is computed using integer arithmetic (k is taken as the integer part of $\dfrac{i+1}{2}$) .

In principle, the larger the value of *N*, the more accurate the numerically inverted solution is. In practice, however, *N* is limited by truncation errors. A characteristic of the V_i's is that their absolute values tend to increase as *N* increases. Thus, the use of large *N* values causes subtraction of one large number from another, with a resulting loss of accuracy. Moench and Ogata (1982) use *N* = 10 and *N* = 18 for their computations. It is a good idea to make the computation with various values of *N* to check if the same result is obtained. High precision arithmetic is usually a necessity. In this study various N values will be tested until a satisfactory result is obtained.

2.4   Verification of the Solution Methods

In order to prove that the applied methods and the subroutine gives satisfactory results, two groundwater flow problems are solved with Laplace transform and numerical inversion by Stehfest algorithm. Then the results are compared against the results which are obtained by analytical inversion.

CHAPTER 3

APPLICATION OF STEHFEST ALGORITHM TO HOMOGENEOUS AQUIFERS

3.1   Introductory Remarks

The main objective of this chapter is to demonstrate how the Stehfest algorithm is used in the solution of groundwater flow problems. For this purpose two problems have been selected. Both of these problems are one dimensional transient flow in a homogeneous aquifer and their exact analytical solutions are available in the literature. These analytical solutions will be used to compare the solutions obtained by Stehfest algorithm. In this chapter a third problem is also solved by Stehfest algorithm. The results of this problem will be used later in the discussion of the flow mechanism in fractured aquifers.

3.2   One dimensional transient flow in a semi-infinite homogeneous aquifer under constant drawdown

The governing partial differential equation for one dimensional transient flow in an aquifer is given as (Bear, 1979) :

$$\frac{\partial^2 h}{\partial x^2} = \frac{1}{\nu}\frac{\partial h}{\partial t} \qquad\qquad (3.1)$$

where;

ν is hydraulic diffusivity

15

h is hydraulic head

x is the distance along the flow direction

t is the time

It is subject to the boundary conditions;

$$h(0,t) = 1 \quad , \quad t>0 \qquad (3.2)$$

$$h(\infty,t) = 0 \quad , \quad t>0 \qquad (3.3)$$

and the initial condition

$$h(x,0) = 0 \quad , \quad x \geq 0 \qquad (3.4)$$

Application of the Laplace transform to each term of (3.1) yields;

$$\frac{\partial^2 \bar{h}}{\partial x^2} = \frac{1}{v}(p\bar{h} - h(x,0)) \qquad (3.5)$$

Replacing the initial condition (3.4) into (3.5) yields;

$$\frac{\partial^2 \bar{h}}{\partial x^2} = \frac{p}{v}\bar{h} \qquad (3.6)$$

Applying the Laplace transform to the boundary conditions (3.2) & (3.3) yields;

$$\bar{h} = \frac{1}{p} \qquad \text{at x=0, and} \qquad (3.7)$$

$$\bar{h} = 0 \qquad \text{as } x \to \infty \qquad (3.8)$$

The general solution of the equation (3.6) is;

$$\bar{h}(x, p) = A\exp(-(p/v)^{0.5}x) + B\exp((p/v)^{0.5}x) \qquad (3.9)$$

A and B are either constants or functions of p (but not x) and are to be determined from boundary conditions. To satisfy (3.3), constant B must be 0. To satisfy (3.2), A must be 1/p. Therefore, the solution of (3.6) subject to (3.2) and (3.3) is;

$$\overline{h}(x,p) = \frac{1}{p}e^{(-(p/v)^{0.5}x)}$$ (3.10)

The solution above is known as the Laplace domain solution. This solution is used in the numerical inversion algorithm (Appendix A) to obtain solution on the real domain.

With this objective, Eq(3.10) is inserted into Eq.(2.12) and this yields;

$$h_n(x,t) \approx (\frac{\ln(2)}{t})\sum_{i=1}^{N}V_i \cdot \frac{1}{p}e^{(-(p/v)^{0.5}x)}$$ (3.11)

In Equ. 3.11, the subscript n for h is used to indicate that the solution is obtained by numerical inversion.

For this problem the analytically inverted solution is available in the literature, which is;

$$h_a(x,t) = erfc(\frac{x}{2\sqrt{v.t}})$$ (3.12)

Similarly in Equ. 3.11, the subscript a for h is used to indicate that the solution is obtained by analytical inversion.

Table 3.1 in the following page summarizes the results obtained for t=4, x=2, v=1 against different N values. Between N=10 and N=20 the results are very close to the exact result, whereas as N gets greater than 20 the numerical method starts to yield unreliable results as demonstrated in the table. In this study N=10 is chosen and used in the solution of other problems, although the results for different N values are compared for the other problems too, their results are omitted from this report. Following the table below an error term is defined against time, and the behaviour of the error as a function of time is examined for N=10. The exact result is independent of N and it is 0.4795.

Table 3.1: Comparison of Numerical results against exact result using different N values.

N	Approximate Result from Numerical Inversion by Stehfest Algorithm	Exact Result from Analytically inverted solution
4	0.4869	
10	0.4795	
20	0.4795	
24	0.4797	0.4795
30	-2.001	
40	$1.2561x10^7$	

3.2.1 Variation of Piezometric Head:
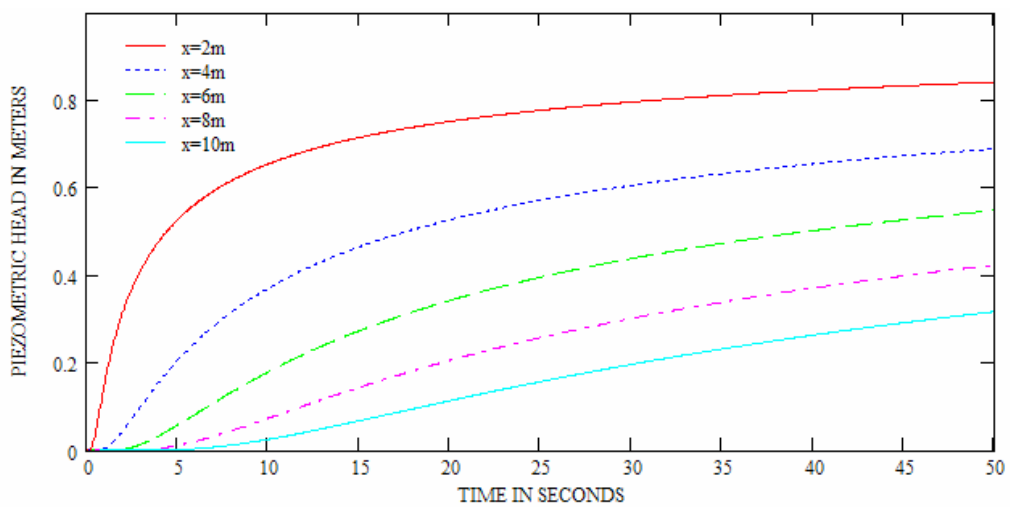
Figure 3.1a: Piezometric head vs time for different values of distance
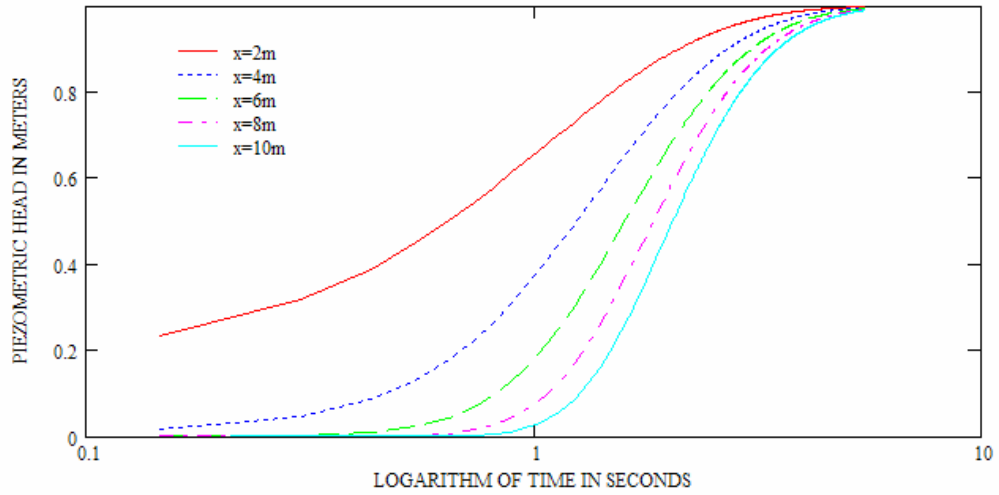
Figure 3.1b: Piezometric head vs log time for different values of distance
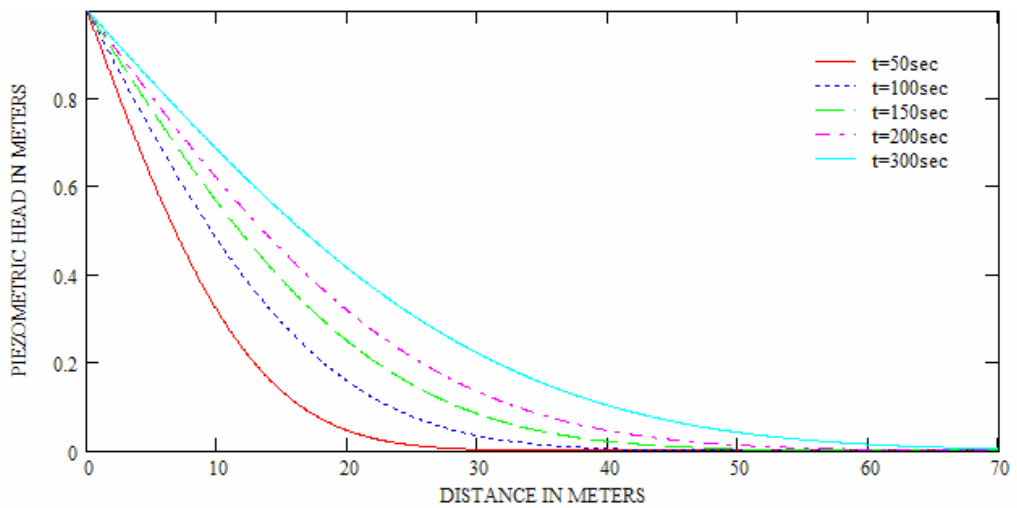
Figure 3.2: Piezometric head vs distance for different values of time

3.2.2 Error Analysis

In order to compare the real results of analytically inverted solution and the results of Stehfest algorithm following error term is defined and plotted against time.

$$E(x,t) = h_n(x,t) - h_a(x,t) \qquad (3.13)$$

Where; $h_n(x,t)$ and $h_a(x,t)$ are the results obtained by numerical and analytical inversion respectively.
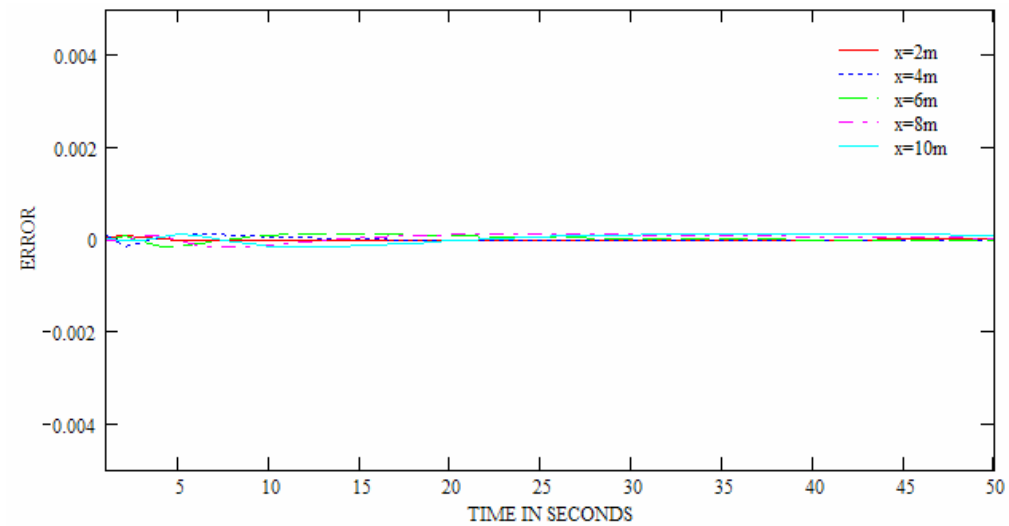
Figure 3.3a: Error function vs. time for different values of distance
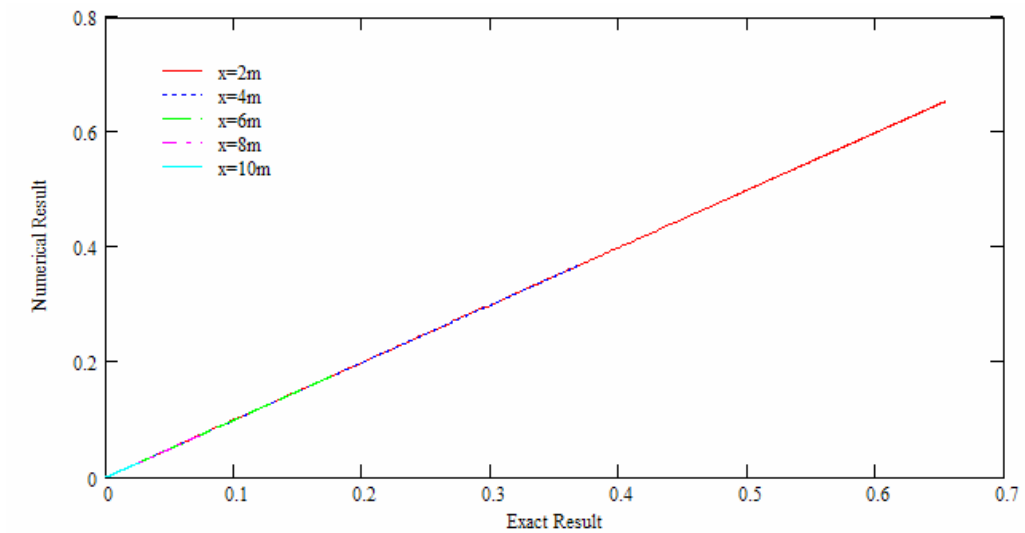
Figure 3.3b: Numerical result vs. exact result for different values of distance x

As it can be seen from the above graphs, the results of the Stehfest algorithm are almost equal to the analytical solution. And the

difference between the results of the numerical solution and the analytical solution are negligible. As expected, the slope of the line in graph 3.3b is 1.

3.3 One dimensional transient flow in a semi-infinite homogeneous aquifer under constant discharge:

The equation (3.1) is the governing one dimensional partial differential equation for this problem too. The only differences are in the boundary conditions as seen below;

Boundary conditions;

$$-LT.\frac{\partial h}{\partial x} = \frac{Q}{2} \qquad \text{at x=0} \tag{3.14}$$

$$h=0 \qquad \text{as } x \to \infty \tag{3.15}$$

and the initial condition

$$h=0 \qquad \text{at t=0} \tag{3.16}$$

where

L is the length of the stream bounding the aquifer

T is the coefficient of transmissivity

Application of the Laplace transform to each term of (3.1) yields

$$\frac{\partial^2 \bar{h}}{\partial x^2} = \frac{1}{v}(p\bar{h} - h(x,0)) \tag{3.17}$$

The initial condition (3.26) yields;

$$\frac{\partial^2 \bar{h}}{\partial x^2} = \frac{p}{v}\bar{h} \tag{3.18}$$

Applying the Laplace transform to the boundary conditions (3.14) &(3.15) yields;

$$-LT.\frac{\partial \overline{h}}{\partial x} = \frac{Q}{2p} \qquad \text{at x=0, and} \qquad (3.19)$$

$$\overline{h} = 0 \qquad \text{as } x \to \infty \qquad (3.20)$$

The general solution of the equation (3.18) is same as (3.9);

$$\overline{h}(x, p) = A\exp(-(p/v)^{0.5} x) + B\exp((p/v)^{0.5} x) \qquad (3.9)$$

To satisfy (3.20), B = 0. And to satisfy (3.19);

$$-LT.A.-(p/v)^{0.5} \exp(-(p/v)^{0.5} x) = \frac{Q}{2p} \qquad (3.21)$$

Hence A is found as;

$$A = \frac{Q}{2LTp.(p/v)^{0.5}} \qquad (3.22)$$

Therefore, the solution of (3.18) subject to (3.19) and (3.20) is ;

$$\overline{h}(x, p) = \frac{Q}{2LTp.(p/v)^{0.5}} e^{(-(p/v)^{0.5} x)} \qquad (3.23)$$

If following variables are defined as, $Q_b = \frac{Q}{L}$ and $Q_d = \frac{Q_b}{T}$; the solution in the Laplace domain will be;

$$\overline{h}(x, p) = \frac{Q_d.v^{0.5}}{2p^{1.5}} e^{(-(p/v)^{0.5} x)} \qquad (3.24)$$

The solution above is known as the Laplace domain solution. Now Laplace inversion needs to be applied to this result to obtain the solution on the real domain as shown in the previous example. For that purpose Eq.(3.24) is inserted into Eq(3.9).

$$h_n(x,t) \approx (\frac{\ln(2)}{t}) \sum_{i=1}^{N} V_i . \overline{h}(x, i\frac{\ln(2)}{t}) \qquad (3.25)$$

Below is the exact solution which is used to compare the results of numerical inversion. (Carslaw & Jaeger, 1959)

$$h_a(x,t) = \frac{Q_d}{2} \left[\left(\sqrt{\frac{4.t.v}{\pi}} \right).e^{\frac{-x}{4.t.v}} + x.(erf(\sqrt{\frac{x^2}{4.t.v}}) - 1 \right] \qquad (3.26)$$

3.3.1 Variation of Piezometric Head:

In the graphics below the variation of the piezometric head is investigated using both the analytical method (the exact solution) and the numerical inversion method. These are compared against each other to find that their results are very close to each other.
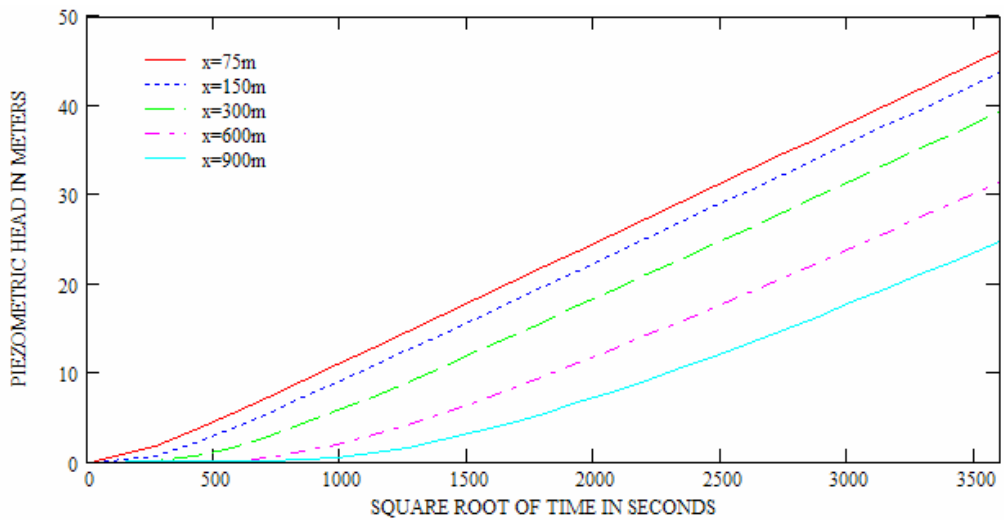
Figure 3.4a: Piezometric head vs. square root of time for different values of distance (Analytical solution formula)
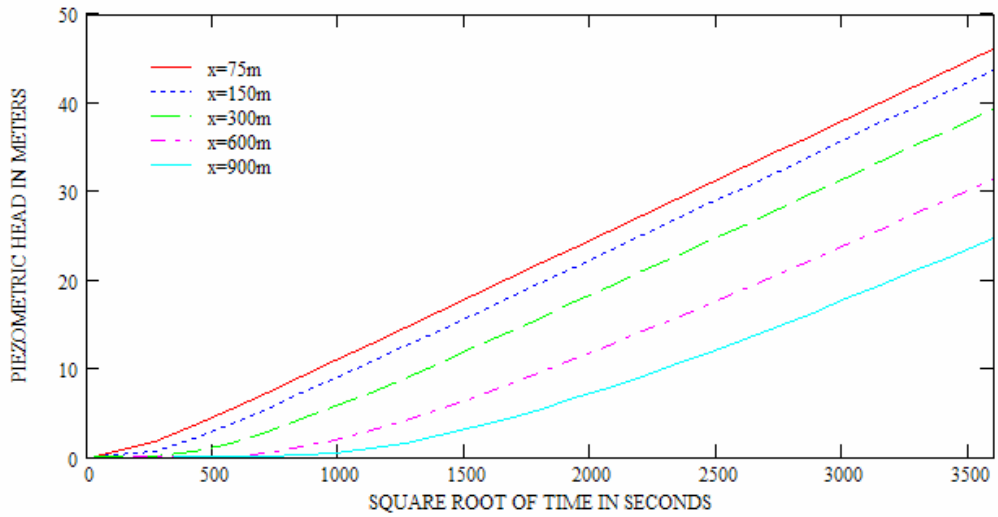
Figure 3.4b: Piezometric head vs. square root of time for different values of distance (Numerical inversion method)

3.3.2 Comparison between analytical and numerical solutions
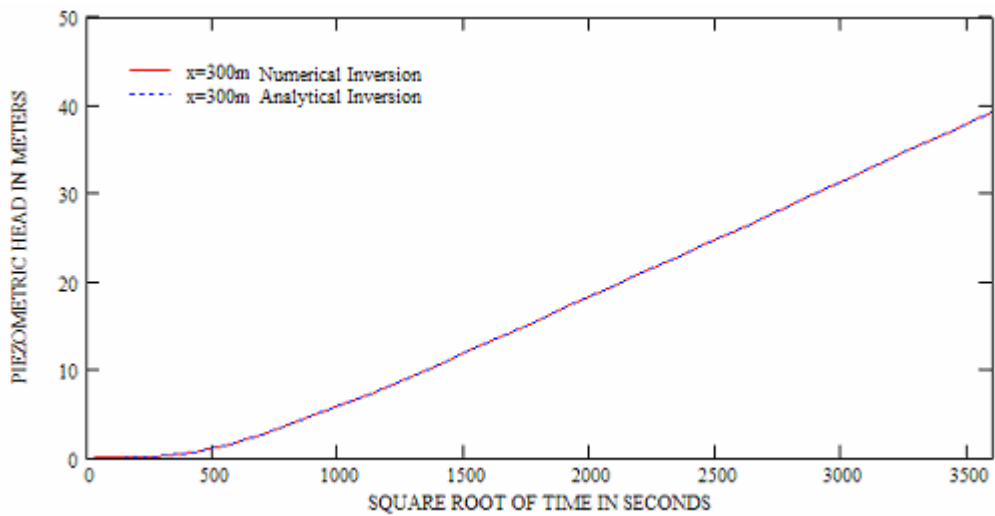
Figure 3.4c: Piezometric head vs. square root of time at x=300m
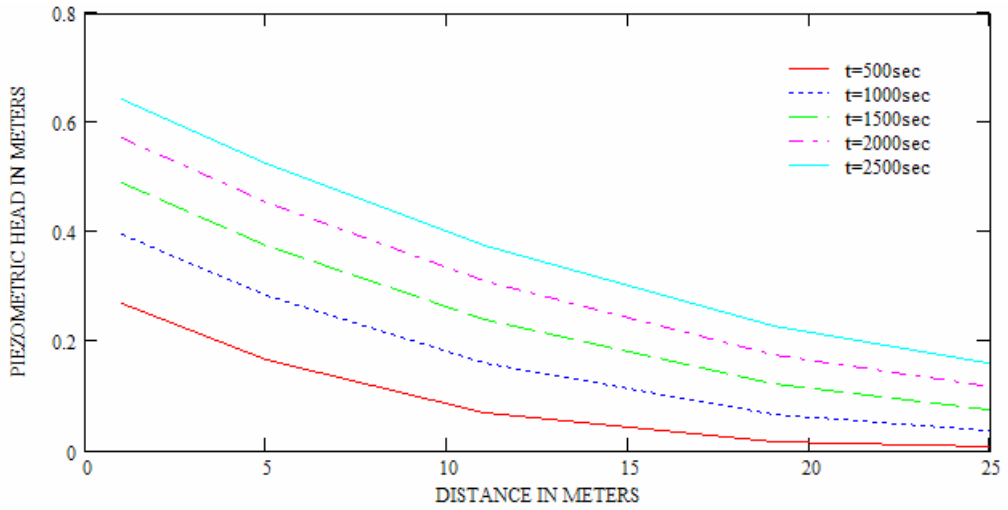
Figure 3.5a: Piezometric head vs. distance for different values of time (Analytical solution formula)
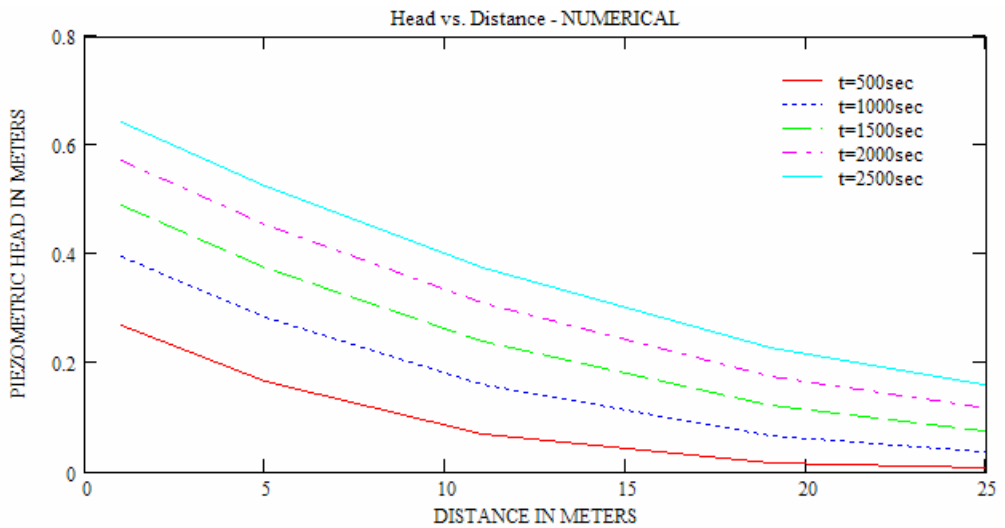
Figure 3.5b: Piezometric head vs. distance for different values of time (Numerical inversion method)
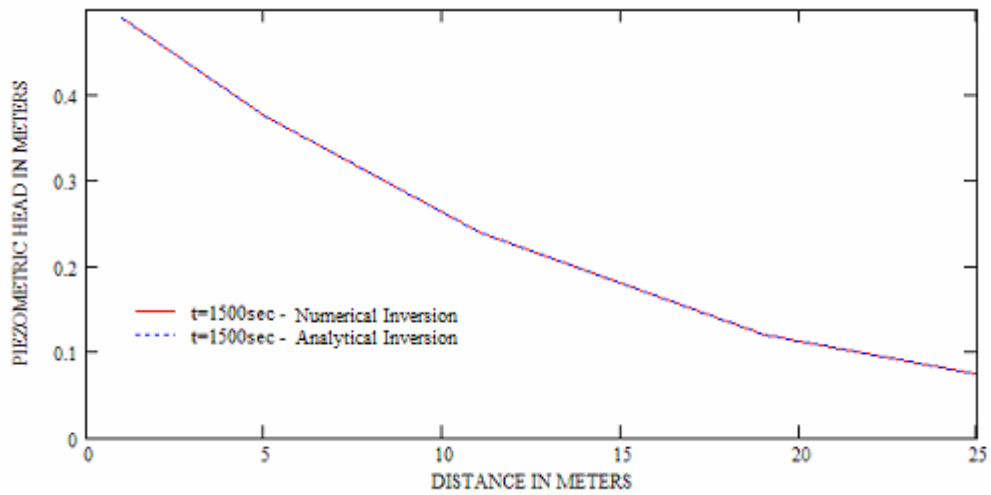
Figure 3.5c: Piezometric head vs. distance at t=1500sec

As it can be seen from the above graphs, the results of the Stehfest algorithm are almost equal to the results of the exact solution.

3.4 One dimensional transient flow in a finite homogeneous aquifer under constant discharge:

The equation (3.1) is the governing one dimensional partial differential equation for this problem too. The only differences are in the boundary conditions as seen below;

Boundary conditions;

$$-LT.\frac{\partial h}{\partial x} = \frac{Q}{2} \qquad \text{at x=0} \qquad (3.27)$$

$$-LT.\frac{\partial h}{\partial x} = 0 \qquad \text{at x=L} \qquad (3.28)$$

and the initial condition

$$h(x,0) = 0 \qquad (3.29)$$

Application of the Laplace transform to each term of (3.1) yields

26

$$\frac{\partial^2 \overline{h}}{\partial x^2} = \frac{p}{\nu}\overline{h}$$ (3.30)

Applying the Laplace transform to the boundary conditions (3.27) &(3.28) yields;

$$-LT.\frac{\partial \overline{h}}{\partial x} = \frac{Q}{2p} \qquad \text{at x=0, and}$$ (3.31)

$$-LT\frac{\partial \overline{h}}{\partial x} = 0 \qquad \text{at } x = L$$ (3.32)

The general solution of the equation (3.30) is;

$$\overline{h}(x,p) = Ae^{-\sqrt{(\frac{p}{\nu})}x} + Be^{\sqrt{(\frac{p}{\nu})}x}$$ (3.33)

Let $\sqrt{\frac{p}{\nu}} = \alpha$ for simplification.

$$\overline{h}(x,p) = Ae^{-\alpha x} + Be^{\alpha x}$$ (3.34)

$$\frac{\partial \overline{h}}{\partial x} = -\alpha Ae^{-\alpha x} + \alpha Be^{\alpha x}$$ (3.35)

Using boundary condition (3.32);

$$0 = -\alpha Ae^{-\alpha L} + \alpha Be^{\alpha L}$$ (3.36)

$$A = Be^{2\alpha L}$$ (3.37)

Replace (3.37) into (3.35) to obtain;

$$\frac{\partial \overline{h}}{\partial x} = -\alpha Be^{2\alpha L}e^{-\alpha x} + \alpha Be^{\alpha x}$$ (3.38)

Simplify (3.38) to obtain;

$$\frac{\partial \overline{h}}{\partial x} = -\alpha B(e^{2\alpha L - \alpha x} - e^{\alpha x})$$ (3.39)

Then replacing second boundary condition (3.32) into (3.39) yields;

$$\frac{Q_d}{2p} = \alpha B(e^{2\alpha L} - 1) \tag{3.40}$$

Solving for B and then $\bar{h}(x, p)$ yields below the Laplace domain solution;

$$B = \frac{Q_d}{2p\alpha(e^{2\alpha L} - 1)} \tag{3.41}$$

$$\bar{h}(x, p) = Be^{2\alpha L}e^{-\alpha x} + Be^{\alpha x} \tag{3.42}$$

The solution above is known as the Laplace domain solution. Laplace inversion needs to be applied to this result to obtain the real solution as shown in the previous examples;

The exact analytical solution for this problem could not be obtained in spite of the extensive literature search. Below graphics are drawn using the results of numerical solution to compare against the semi-infinite version of the problem.

3.4.1 Comparison of the Results:

Below constants are considered for the hypothetical finite homogeneous aquifer to carry out the numerical inversion procedure;

$$v = 0.135 \qquad Q_d = 0.065 \qquad S = 2.10^{-5} \qquad T = 2.7.10^{-6} m^2 / \sec$$

$$L = 100m \qquad \text{where } v = \frac{T}{S}$$
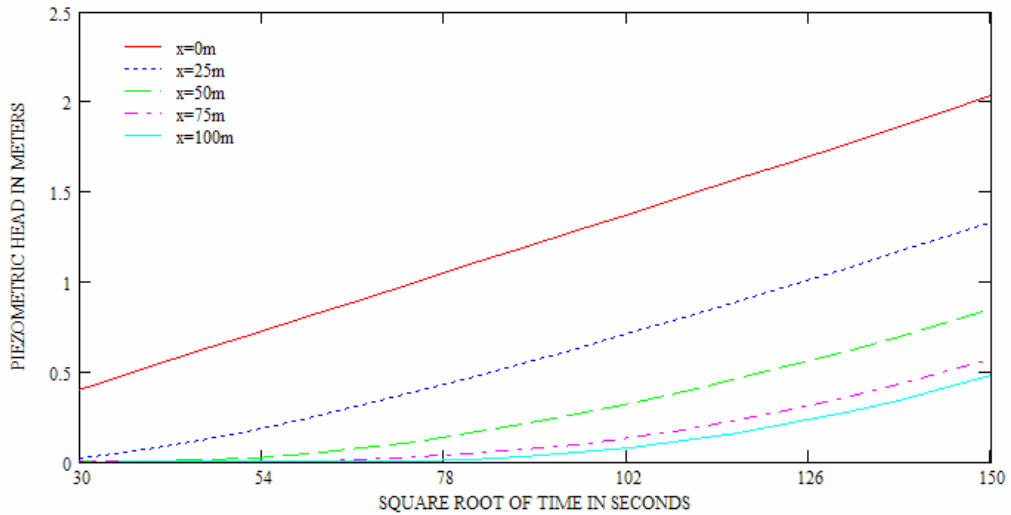
Figure 3.6a: Piezometric head vs. square root of time for different values of distance - Finite H. Aquifer
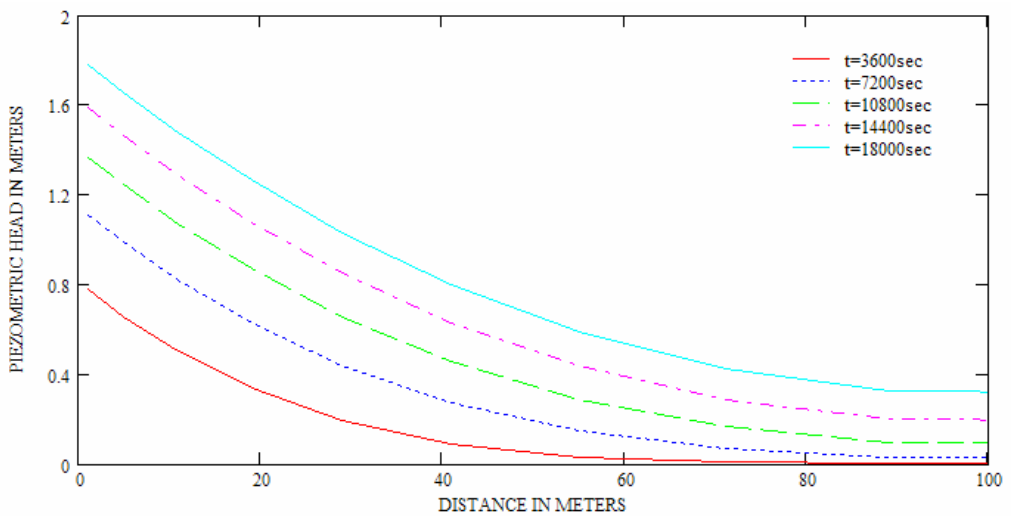
Figure 3.6b: Piezometric head vs. distance for different values of time – Finite H. Aquifer

Below graphics are results for the semi-infinite case of the problem. The same parameters and boundaries are used for both cases to make the comparison.
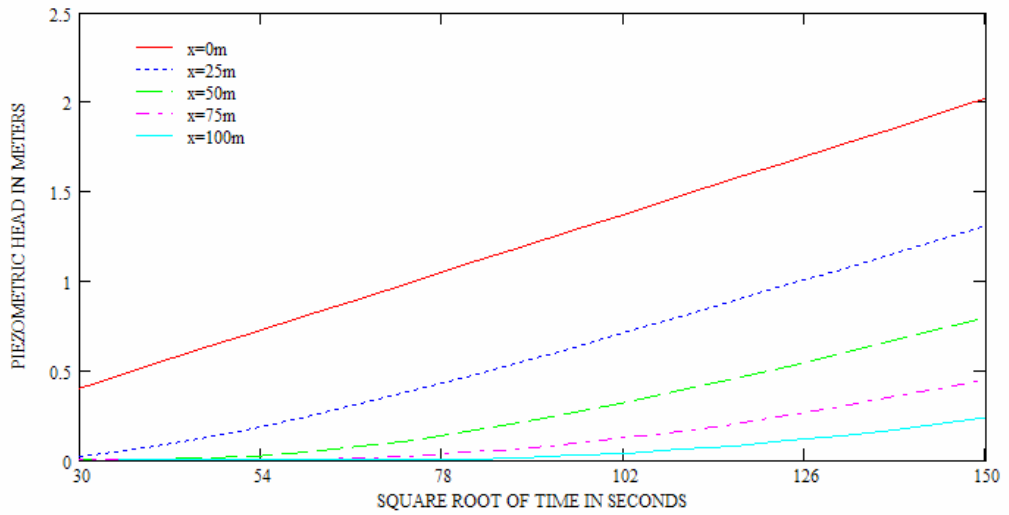
Figure 3.7a: Piezometric head vs. square root of time at for different values of distance - Semi-infinite H. Aquifer
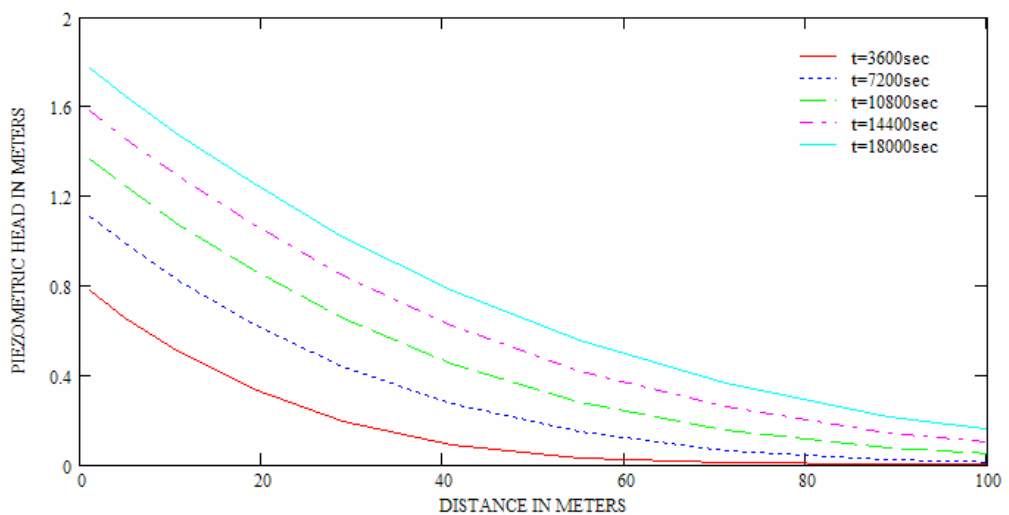
Figure 3.7b: Piezometric head vs. distance for different values of time - Semi-infinite H. Aquifer

The behavior of the piezometric head in both semi-infinite and finite homogeneous aquifers is plotted together for several selected values of time and distance for comparison.
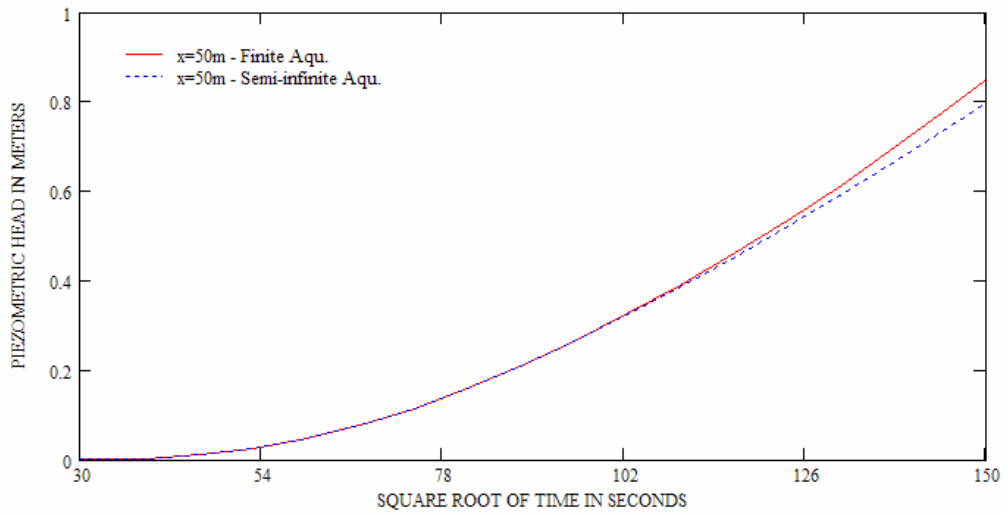
Figure 3.8a: Piezometric head vs. square root of time at x=50m – (Finite and Semi-Infinite Aquifers)
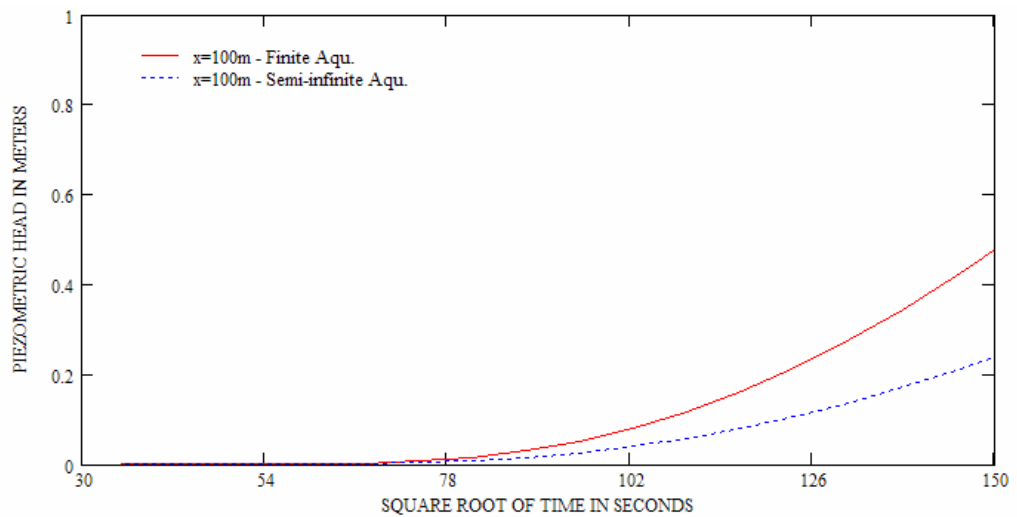
Figure 3.8b: Piezometric head vs. square root of time at x=100m – (Finite and Semi-Infinite Aquifers)

31
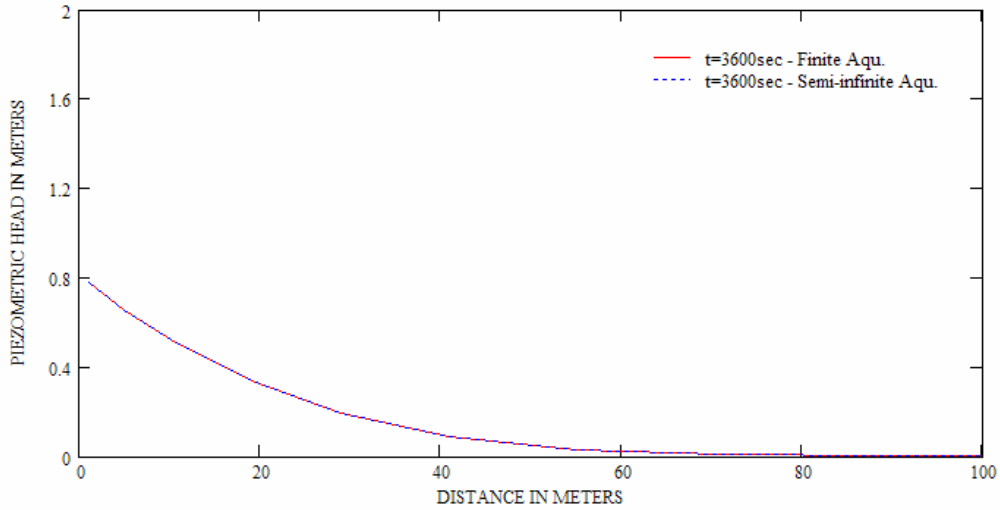
Figure 3.9a: Piezometric head vs. distance at t=3600sec – (Finite and Semi-Infinite Aquifers)
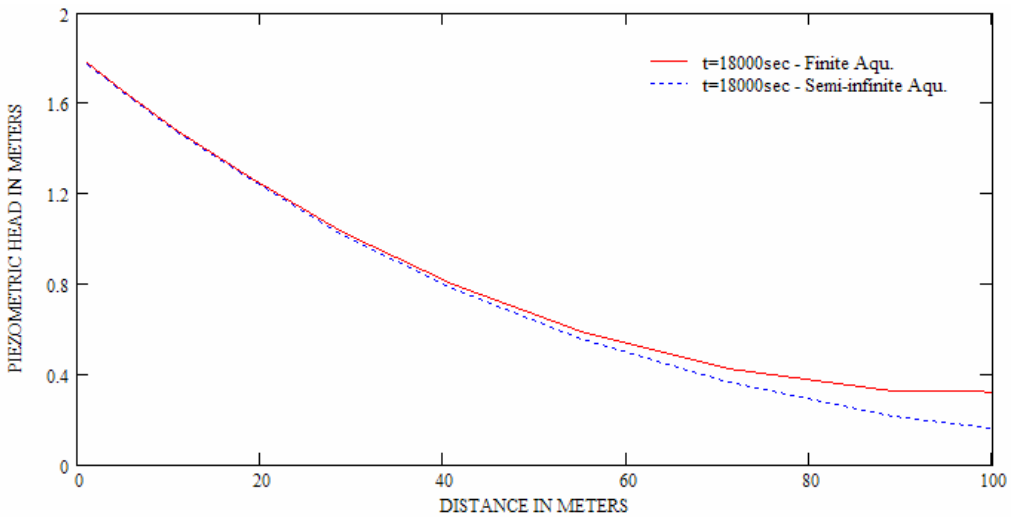
Figure 3.9b: Piezometric head vs. distance at t=18000sec – (Finite and Semi-Infinite Aquifers)

As it can be seen from the graphics above, the behavior of the piezometric head is the similar for both semi-infinite and finite cases for short distance and in a short period of time. As the time increases (discharge from the river continues) the piezometric head in the finite aquifer starts to increase more rapidly then the semi-infinite aquifer case. Also as the distance increases; the difference between the

piezometric heads of semi-infinite and finite homogeneous aquifers increases where the head in the finite aquifer is always higher.

CHAPTER 4

APPLICATION OF STEHFEST ALGORITHM TO FRACTURED AQUIFERS

4.1 Solution Procedure

First of all the differential equations and the boundary conditions are non-dimensionalized to make it simpler to draw graphics and compare the variables. The second step is transferring all the boundary conditions and the differential equations to Laplace domain –applying Laplace transform- which is followed by the analytical solution of the differential equations in Laplace domain. Then the solutions in Laplace domain are converted to real domain with the help of a numerical tool: Stehfest Algorithm.

4.2 One dimensional transient flow in a semi-infinite fractured aquifer with constant discharge

In order to non-dimensionalize the equations 2.1 to 2.10 following transformations are applied to these equations;

$$z_1 = \frac{h_0 - h_1}{h_0} \tag{4.1}$$

$$z_2 = \frac{h_0 - h_2}{h_0} \tag{4.2}$$

$$y = \frac{x}{h_0} \tag{4.3}$$

$$\theta = \frac{T_1 t}{S_1 h_o^{\,2}} \tag{4.4}$$

where;

z_1 is the dimensionless head in fractures

z_2 is the dimensionless head in blocks

y is the dimensionless distance from the face of the stream

θ is the dimensionless time.

Using the equations (3.1)-(3.4) the following non-dimensional equations are obtained;

$$\frac{\partial^2 h_1}{\partial x^2} = -\frac{\partial^2 z_1}{h_0 \partial y^2}$$ (4.5)

$$\frac{\partial h_1}{\partial t} = -\frac{T_1}{S_1 h_0}\frac{\partial z_1}{\partial \theta}$$ (4.6)

$$\frac{\partial h_2}{\partial t} = -\frac{T_1}{S_1 h_0}\frac{\partial z_2}{\partial \theta}$$ (4.7)

If (4.5)-(4.7) is replaced into (2.1) & (2.2) the following equations are obtained;

$$\frac{\partial^2 z_1}{\partial y^2} = \frac{\partial z_1}{\partial \theta} + \eta \frac{\partial z_2}{\partial \theta}$$ (4.8)

$$\frac{\partial z_2}{\partial \theta} = \delta(z_1 - z_2)$$ (4.9)

where

$$\delta = \frac{S_1}{T_1}\frac{T_2}{S_2}\varepsilon h_0^2 \qquad \text{and} \qquad \eta = \frac{S_2}{S_1}$$ (4.10)

Similarly the initial and the boundary conditions are:

$z_1(y.0)=0$ (4.11)

$z_2(y.0)=0$ (4.12)

$$\lim_{y \to 0}\frac{\partial z_1}{\partial y} = -Q_d$$ (4.13)

35

$$\lim_{y \to \infty} z_1 = 0 \tag{4.14}$$

Where the dimensionless discharge Q_d is defined as:

$$Q_d = \frac{Q_b}{T_1} \tag{4.15}$$

If the Laplace Transform is applied to the equations (4.8) & (4.9) then;

$$\frac{\partial^2 \bar{z}_1}{\partial y^2} = p\bar{z}_1 + \eta p \bar{z}_2 \tag{4.16}$$

$$p\bar{z}_2 = \delta(\bar{z}_1 - \bar{z}_2) \tag{4.17}$$

If the Laplace Transform is applied to the initial and boundary conditions (4.11) to (4.14) then;

$$\bar{z}_1 = 0 \quad \text{at y=0} \tag{4.18}$$

$$\bar{z}_2 = 0 \quad \text{at y=0} \tag{4.19}$$

$$\lim_{y \to 0} \frac{\partial \bar{z}_1}{\partial y} = -Q_d \cdot \frac{1}{p} \tag{4.20}$$

$$\lim_{y \to \infty} \bar{z}_1 = 0 \tag{4.21}$$

Now (4.17) can be solved for $\bar{z}_2$ to obtain;

$$\bar{z}_2 = \frac{\delta \bar{z}_1}{p + \delta} \tag{4.22}$$

Replacing (4.22) into (4.16) yields;

$$\frac{\partial^2 \bar{z}_1}{\partial y^2} = p\bar{z}_1 + \eta p \frac{\delta \bar{z}_1}{p + \delta} \tag{4.23}$$

$$\frac{\partial^2 \bar{z}_1}{\partial y^2} - (p + \frac{p\eta\delta}{p + \delta})\bar{z}_1 = 0 \tag{4.24}$$

Equation (4.24) is in the form of $(D^2 - \alpha^2)\bar{z}_1 = 0$

D is $\dfrac{\partial^2 ()}{\partial y^2}$ and α is $(p + \dfrac{p\eta\delta}{p+\delta})$ therefore;

$$D_1 = +\sqrt{p + \frac{p\eta\delta}{p+\delta}} \qquad (4.25a)$$

$$D_2 = -\sqrt{p + \frac{p\eta\delta}{p+\delta}} \qquad (4.25b)$$

$$\bar{z}_1 = Ae^{D_1 y} + Be^{D_2 y} \qquad (4.26)$$

Using the Boundary Condition (4.21); $\qquad\qquad\qquad A = 0$

Using the Boundary Condition (4.20); $\qquad\qquad\qquad B = -\dfrac{Q_d}{pD_2}$

$$\bar{z}_1(y,p) = +\frac{Q_d}{p\sqrt{p + \dfrac{p\eta\delta}{p+\delta}}}\, e^{D_2 y} \qquad (4.27)$$

$$\bar{z}_2(y,p) = +\frac{\delta Q_d}{p}\frac{1}{\sqrt{p + \dfrac{p\eta\delta}{p+\delta}}}\frac{1}{(p+\delta)}\, e^{D_2 y} \qquad (4.28)$$

Now two solutions have been obtained for the two equations in Laplace Domain for the semi-infinite fractured aquifer problem. In order to get the results in the real domain numerical inversion should be applied as follows:

By inserting Eq. (4.27) into Eq.(2.12) z_1 is obtained as:

$$z_1(y,\theta) \approx (\frac{\ln(2)}{\theta})\sum_{i=1}^{N} V_i.\bar{z}_1(y,i\frac{\ln(2)}{\theta}) \qquad (4.29)$$

Similarly by inserting Eq. (4.28) into Eq.(2.12) z_2 is obtained as:

$$z_2(y,\theta) \approx (\frac{\ln(2)}{\theta})\sum_{i=1}^{N} V_i.\bar{z}_2(y,i\frac{\ln(2)}{\theta}) \qquad (4.30)$$

In order to check the validity of the results, the methods utilized over the course of this study are used to solve other groundwater problems as demonstrated in Chapter 3 and these results are compared against the exact solution. However the problems considered in this chapter have not been solved analytically before; so the exact solutions for these problems are not available in the literature.

Following parameter values and aquifer constants are considered for the hypothetical aquifer to illustrate the behavior of the groundwater flow :

$$v = 0.135 m^2 / \sec \qquad Q_d = 0.065 \qquad S_1 = 2.10^{-5} \qquad T_1 = 2.7.10^{-6} m^2 / \sec$$

$$\eta = 5 \qquad\qquad \delta = 0.625$$

where $v = \dfrac{T_1}{S_1}$
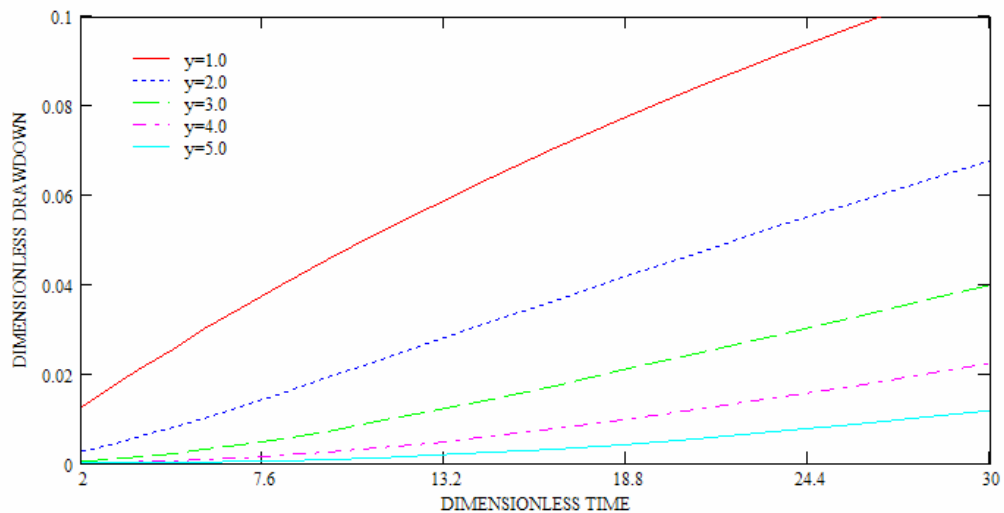
Figure 4.1: Dimensionless drawdown z_1 vs dimensionless time θ for different values of dimensionless distance y – Semi Infinite Fractured Aquifer
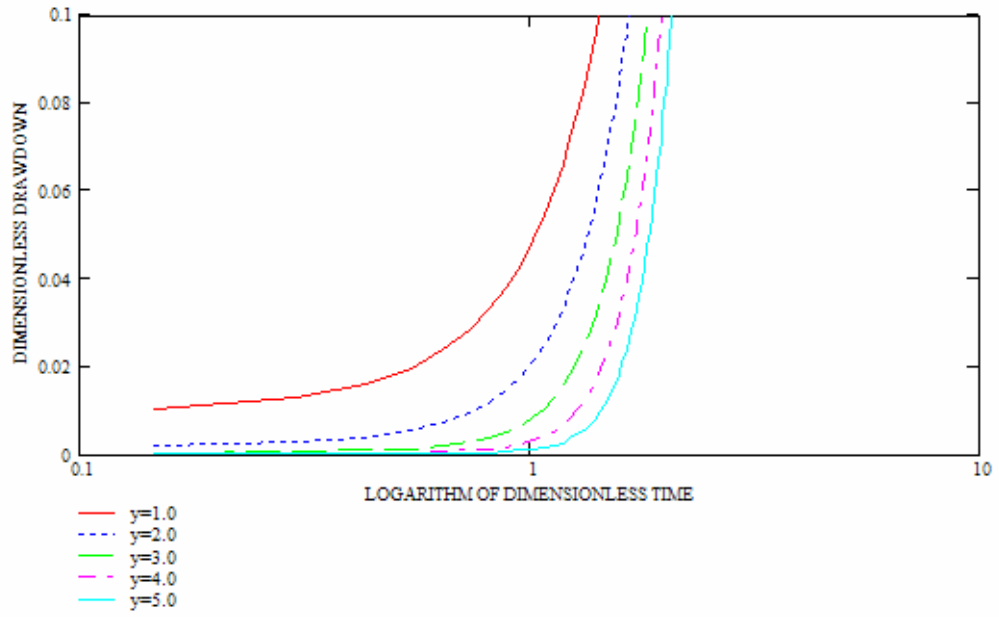
Figure 4.2: Dimensionless drawdown z_1 vs logarithm of dimensionless time θ for different values of dimensionless distance y – Semi Infinite Fractured Aquifer
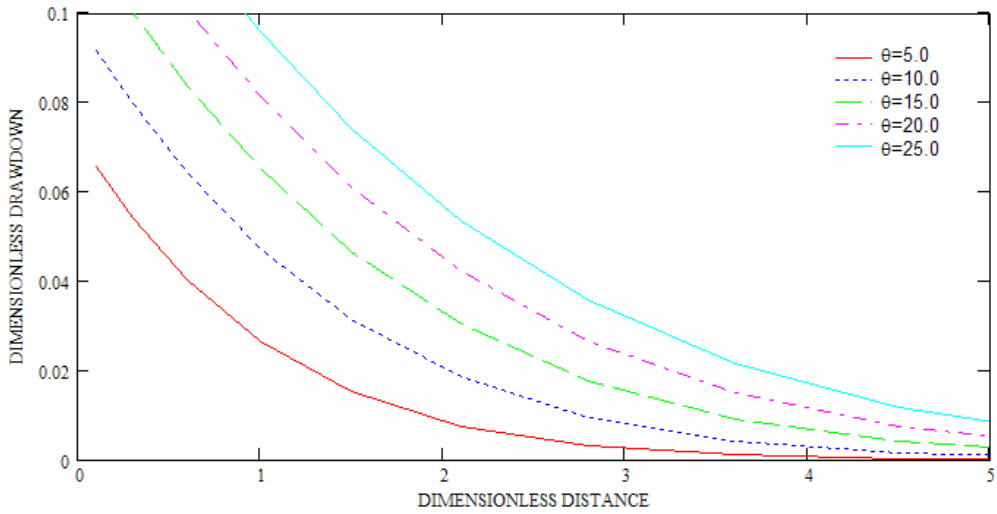
Figure 4.3: Dimensionless drawdown z_1 vs dimensionless distance y for different values of dimensionless time θ – Semi Infinite Fractured

Figure 4.4: Dimensionless drawdown z_1 vs. logarithm of dimensionless time θ for different values of η where y=1 δ=5 Semi Infinite Fractured Aquifer

Figure 4.5: Dimensionless drawdown z_1 vs. logarithm of dimensionless time θ for different values of δ where y=1 η=5 Semi Infinite Fractured Aquifer

4.3 One dimensional transient flow in a finite fractured aquifer with constant discharge

The governing differential equations are exactly the same as the equations for the previous case except the boundary conditions.

The solution will again be in the form of;

$$\bar{z}_1 = Ae^{D_1 y} + Be^{D_2 y} \qquad (4.31)$$

$$\frac{\partial \bar{z}_1}{\partial y} = D_1 Ae^{D_1 y} + D_2 Be^{D_2 y} \qquad (4.32)$$

where D_1 and D_2 are defined by Eq 4.25a and 4.25b

$$D_{1,2} = \mp \sqrt{p + \frac{p\eta\delta}{p + \delta}} \qquad (4.33)$$

Initial conditions:

$z_1 = 0$ at y=0 $\qquad (4.34)$

$z_2 = 0$ at y=0 $\qquad (4.35)$

The boundary conditions will be as follows;

$$\lim_{y \to 0} \frac{\partial z_1}{\partial y} = -Q_d \qquad (4.36)$$

$$\lim_{y \to \frac{L}{h_0}} \frac{\partial z_1}{\partial y} = 0 \qquad (4.37)$$

If Laplace Transform is applied to the initial and boundary conditions (4.34) to (4.37) following relationships will be obtained;

$\bar{z}_1 (y.0)=0 \qquad (4.38)$

$\bar{z}_2 (y.0)=0 \qquad (4.39)$

$$\lim_{y \to 0} \frac{\partial \bar{z}_1}{\partial y} = -\frac{Q_d}{p} \tag{4.40}$$

$$\lim_{y \to \frac{L}{h_0}} \frac{\partial \bar{z}_1}{\partial y} = 0 \tag{4.41}$$

Using the boundary condition (4.40);

$$-\frac{Q_d}{p} = D_1 A + D_2 B \tag{4.42}$$

Solving (4.41) for A yields;

$$A = (-\frac{Q_d}{p} - D_2 B)\frac{1}{D_1} \tag{4.43}$$

Similarly using the boundary condition (4.41);

$$0 = D_1 A e^{D_1 \frac{L}{h_0}} + D_2 B e^{D_2 \frac{L}{h_0}} \tag{4.44}$$

Then (4.43)is replaced in (4.44) to obtain;

$$0 = (-\frac{Q_d}{p} - D_2 B)e^{D_1 \frac{L}{h_0}} + D_2 B e^{D_2 \frac{L}{h_0}} \tag{4.45}$$

Solving (4.45) for B yields;

$$B = \frac{Q_d}{p} \frac{e^{D_1 \frac{L}{h_0}}}{D_2 (e^{D_2 \frac{L}{h_0}} - e^{D_1 \frac{L}{h_0}})} \tag{4.46}$$

Hence the solution for $\bar{z}_1$ in the Laplace domain will be obtained by replacing A (Eq. 4.43) and B (Eq. 4.46) into Eq. (4.31);

$$\bar{z}_1(y, p) = (-\frac{Q_d}{p} - D_2 B)\frac{1}{D_1}e^{D_1 y} + B e^{D_2 y} \tag{4.47}$$

Similarly $\bar{z}_2$ is obtained as:

$$\bar{z}_2(y,p) = \frac{\delta}{p+\delta}[(-\frac{Q_d}{p} - D_2 B)\frac{1}{D_1}e^{D_1 y} + Be^{D_2 y}] \qquad (4.48)$$

Stehfest Algorithm is used as shown below to invert the solution in the Laplace domain above and to obtain the solution in the real domain;

By inserting Eq. (4.47) into Eq.(2.12) z_1 is obtained as:

$$z_1(y,\theta) \approx (\frac{\ln(2)}{t})\sum_{i=1}^{N} V_i.\bar{z}_1(y,i\frac{\ln(2)}{\theta}) \qquad (4.49)$$

Similarly by inserting Eq. (4.48) into Eq.(2.12) z_2 is obtained as:

$$z_2(y,\theta) \approx (\frac{\ln(2)}{t})\sum_{i=1}^{N} V_i.\bar{z}_2(y,i\frac{\ln(2)}{\theta}) \qquad (4.50)$$

Below constants are considered for the hypothetical aquifer to carry out the numerical inversion procedure;

$$v = 0.135 \qquad Q_d = 0.065 \qquad S_1 = 2.10^{-5} \qquad T_1 = 2.7.10^{-6} m^2/\sec \quad \eta = 5$$

$$\delta = 0.625 \qquad L = 100m \qquad h_0 = 20m \text{ where } v = \frac{T_1}{S_1}$$
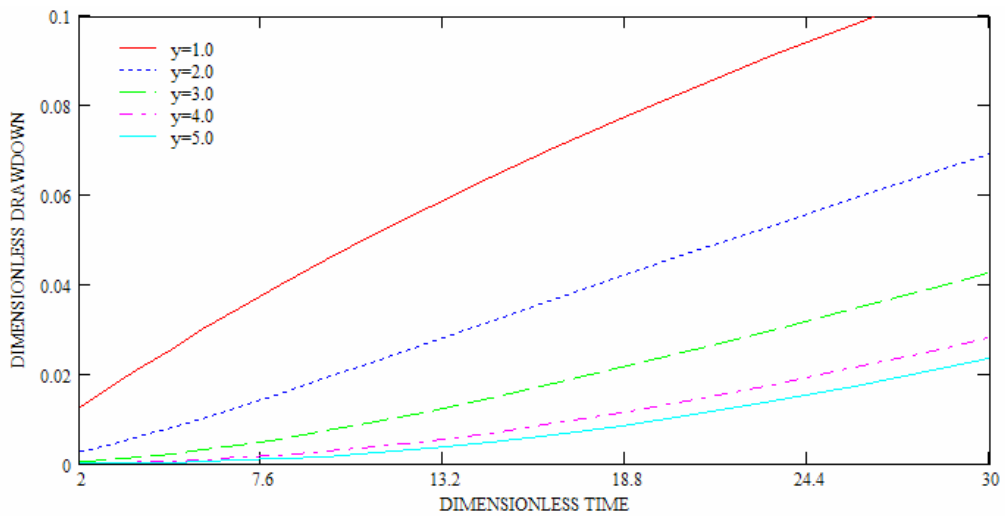
Figure 4.6: Dimensionless drawdown z_1 vs. dimensionless time θ for different values of y - Finite Fractured Aquifer
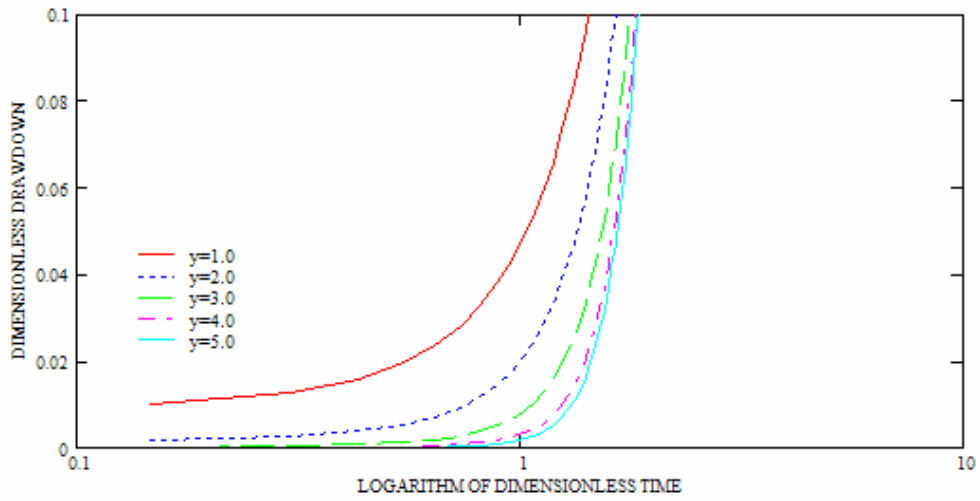
Figure 4.7: Dimensionless drawdown z_1 vs. logarithm of dimensionless time θ for different values of y - Finite Fractured Aquifer

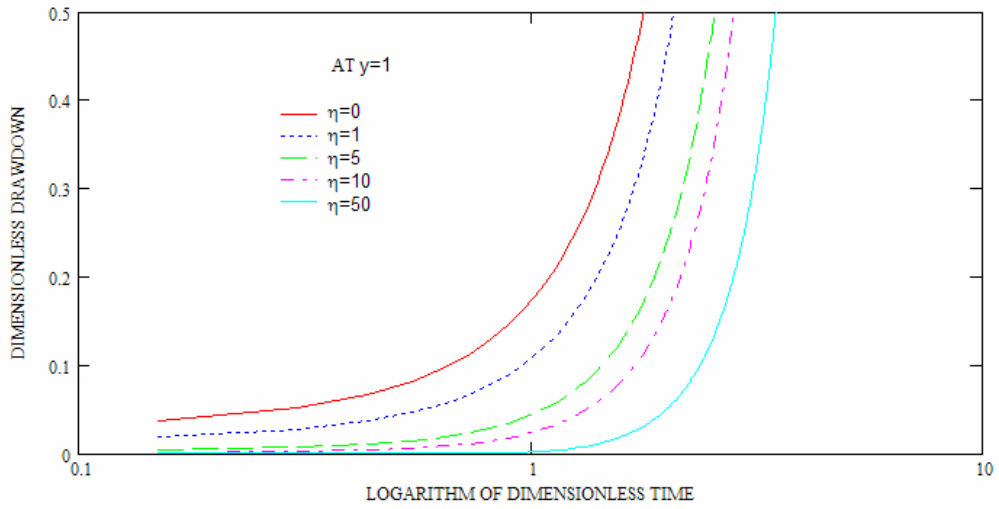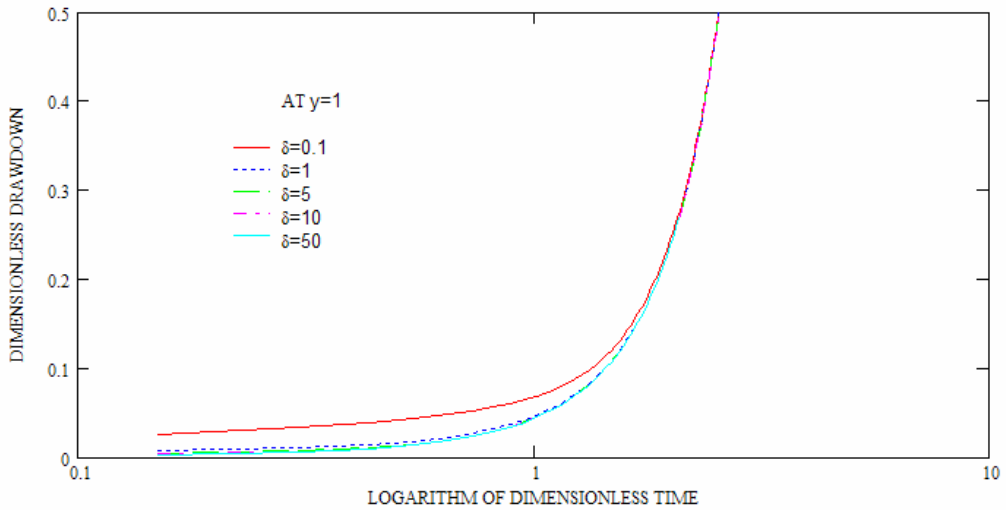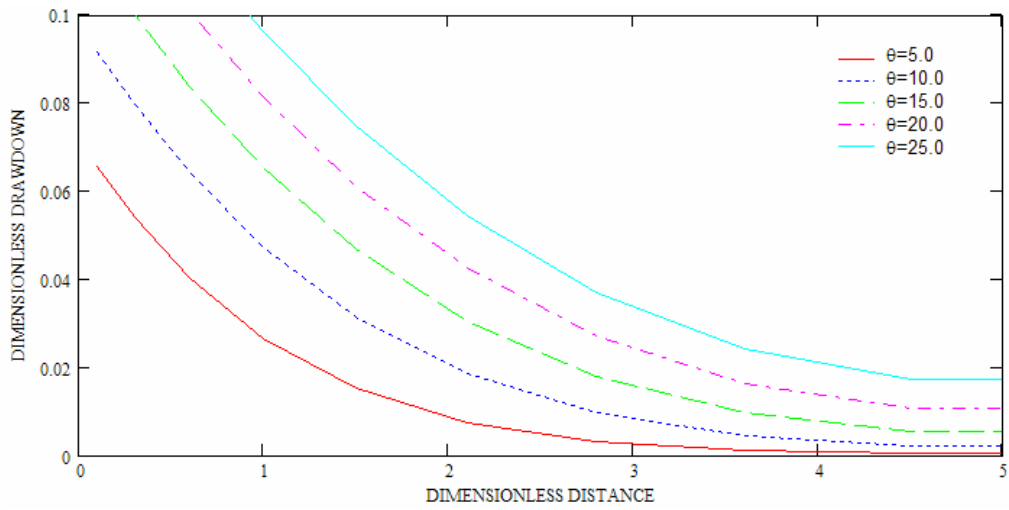Figure 4.8: Dimensionless drawdown z_1 vs. dimensionless distance y for different values of θ - Finite Fractured Aquifer
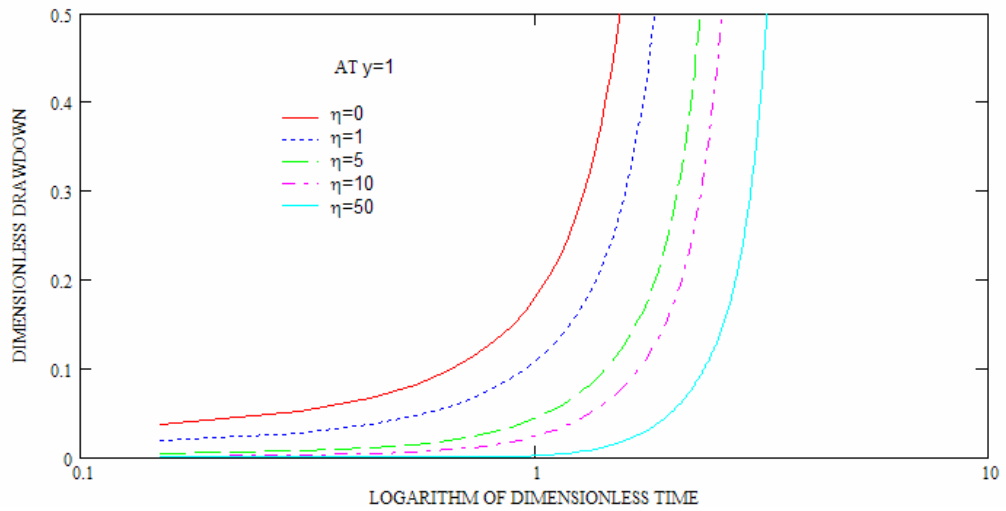
Figure 4.9: Dimensionless drawdown z_1 vs. logarithm of dimensionless time θ for different values of η where y=1 δ=5 Finite Fractured Aquifer
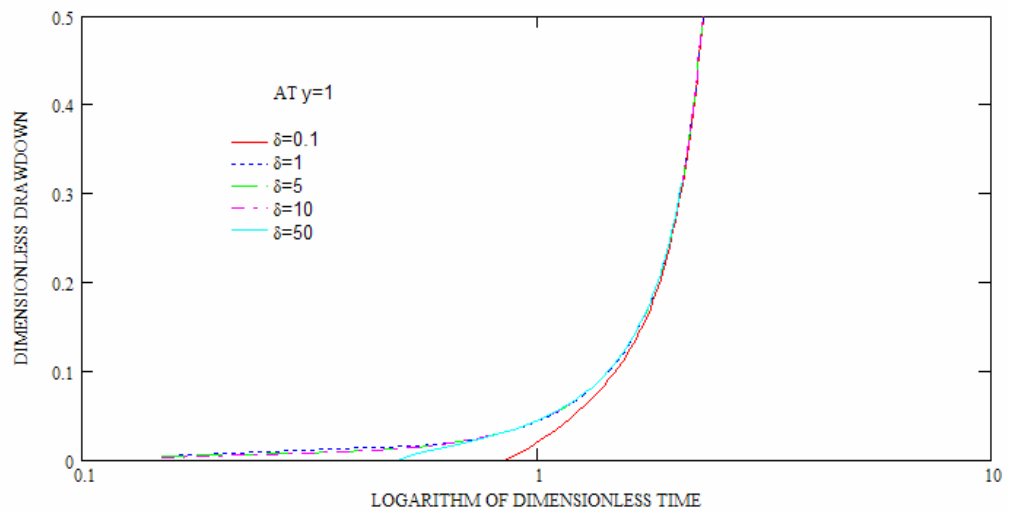
Figure 4.10: Dimensionless drawdown z_1 vs. logarithm of dimensionless time θ for different values of δ where y=1 η=5 - Finite Fractured Aquifer

45
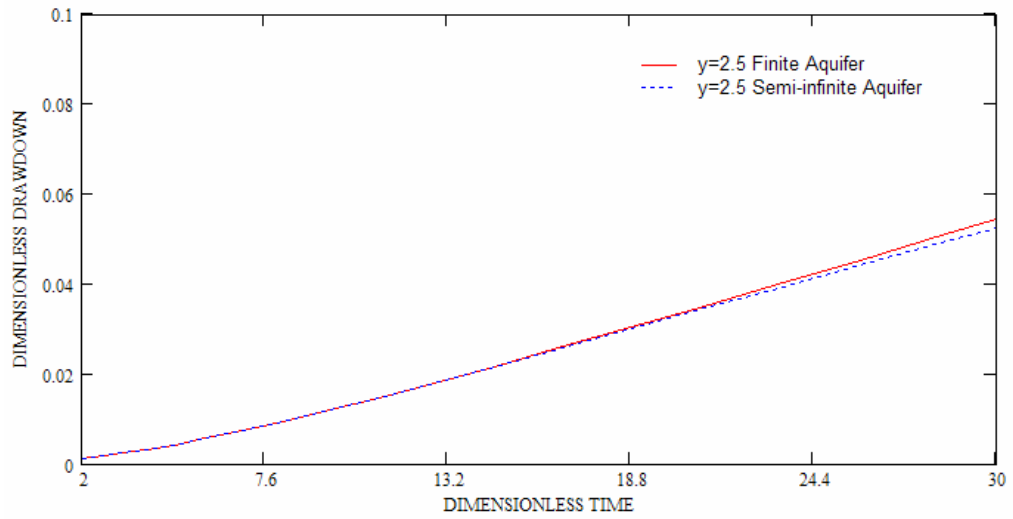
Figure 4.11a: Dimensionless Drawdown vs. dimensionless time at y=2.5
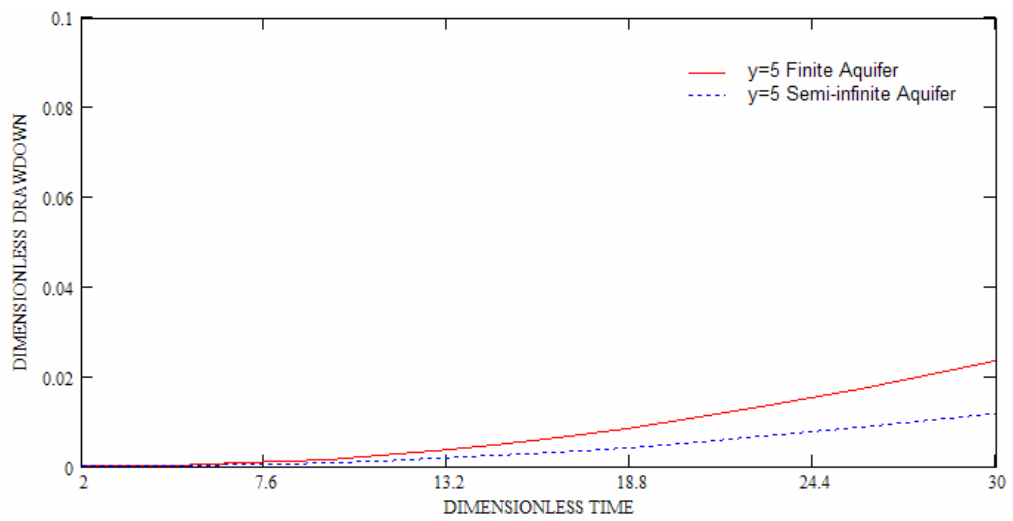
Figure 4.11b: Dimensionless Drawdown vs. dimensionless time at y=5
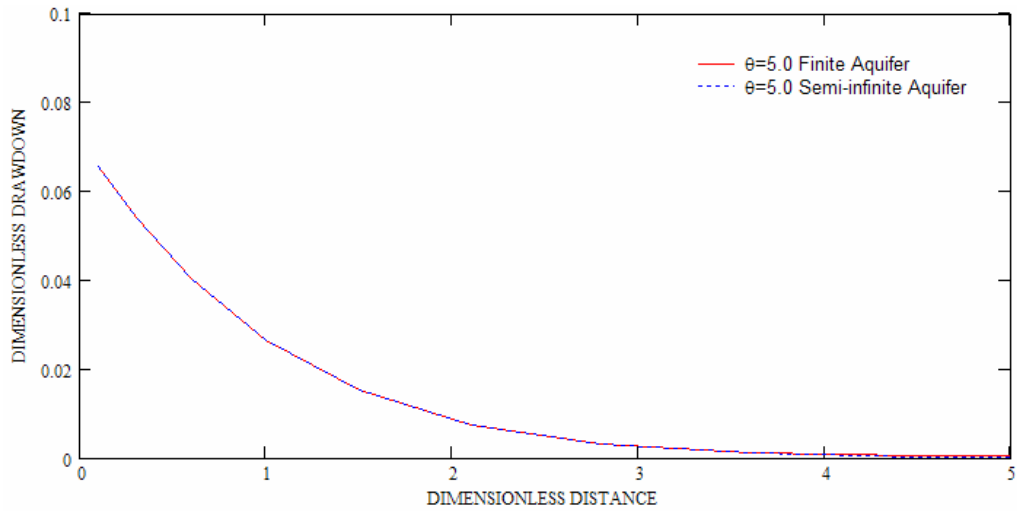
Figure 4.12a: Dimensionless drawdown vs. dimensionless distance at θ=5
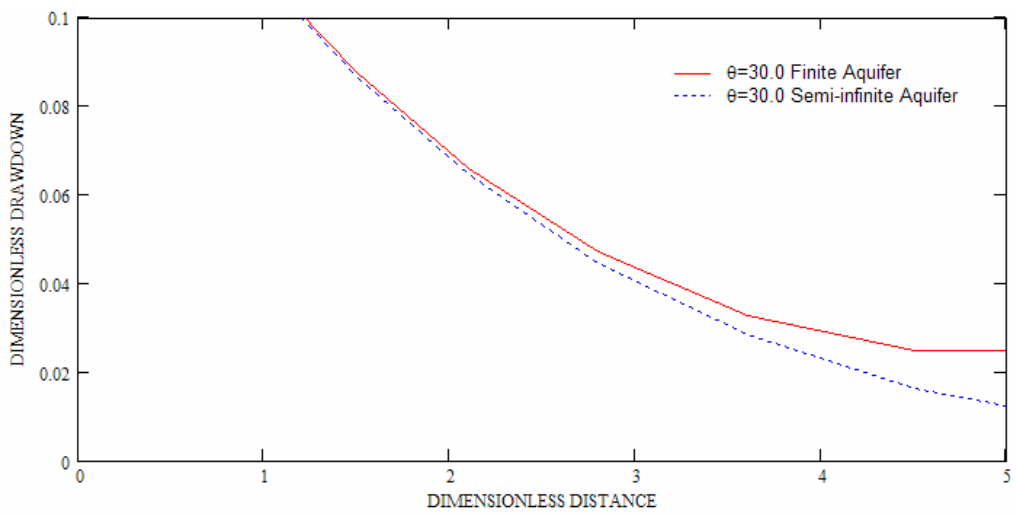
Figure 4.12b: Dimensionless drawdown vs. dimensionless distance (y) at θ=30

As expected, the dimensionless drawdown vs. dimensionless time graphics of both finite and infinite cases is following exactly the same pattern. The graphics are drawn for a range of 0-100m and 30min-6hours of discharge. Unfortunately as the time value increases in the finite fracture case the numerical solution does not yield an answer

because of very big numbers. Such as some of the parameters in the series becoming greater than 10^307, and the software stops carrying out the calculations after these values. As shown in the previous chapter the graphs of the two cases are expected to start separating after a point for greater values of dimensionless distance and dimensionless time. As an alternative method of comparison the finite fractured and semi-infinite fractured cases are analysed in detail using the Ferris equations in the following chapter.

CHAPTER 5

INTERPRETATION AND DISCUSSION OF RESULTS

5.1 Introduction

The objective in this chapter is to explore the behavior of groundwater flow in fractured aquifers. This objective includes also the comparison of the responses of groundwater flow in fractured and homogeneous aquifers of same geometry to the imposed boundary and initial conditions of the same type. Finally a comparison between the results for the flow in semi-infinite and finite fractured aquifer is also considered in this chapter.

5.2 Results of Semi-infinite Fractured Aquifer

Two dimensionless parameters are defined in the presentations of the results as follows;

$$u(x,t) = x\sqrt{\frac{S_1}{4T_1 t}}$$
(5.1)

Note that this dimensionless variable is commonly used in groundwater literature and it may be related to the dimensionless quantities used earlier in Chapter 4 in the present study:

$$u(x,t) = \frac{y}{2\sqrt{\theta}}$$
(5.2)

$$D(u) = D(z, y) = \frac{z_1}{Q_d \cdot y} \tag{5.3}$$

where z_1 is found from the numerical inversion method as demonstrated in chapter 4, Eq. 4.29. A subroutine - which can be found in Appendix C.1- is written to draw $D(u)$ vs. $u^2(x,t)$ by using the numerical solution method.

For the semi-infinite homogeneous aquifer with constant discharge problem based on Ferris et al. (1962) the function D,u,z are defined by Lohman (1972) as,

$$u(x,t) = x\sqrt{\frac{S}{4Tt}} \tag{5.4}$$

$$D(u) = \frac{e^{-u^2}}{u.\sqrt{\pi}} - 1 + erf(u) \tag{5.5}$$

$$z(x) = Q_d x.D \tag{5.6}$$

where z(x,t) is the exact analytical solution known as Ferris' equation, and D(u) is also known as the drain function of u. Subroutine written to draw $D(u)$ vs. $u^2(x,t)$ can be found in Appendix C.2-

In order to compare the results of the exact solution against the solution obtained by numerical inversion for the homogeneous problem; z is calculated from the Stehfest algorithm (as demonstrated in Chapter 2) and then it is used to calculate $u(x,t)$ and $D(u)$

$z_1(x)$ is calculated by numerical inversion $\tag{5.7}$

The subroutine used to draw $D(u)$ vs. $u^2(x,t)$ for semi-infinite homogeneous aquifer with constant discharge problem by using the numerical inversion method can be found in Appendix C.3.

The constants below are used to draw the graphics in this chapter

$$v = 0.135 \qquad Q_d = 0.065 \qquad S_1 = 2.10^{-6} \qquad T_1 = 2.10^{-7}\, m^2/\sec \qquad \eta = 5$$

$$\delta = 0.625 \qquad \text{where } v = \frac{T_1}{S_1}$$
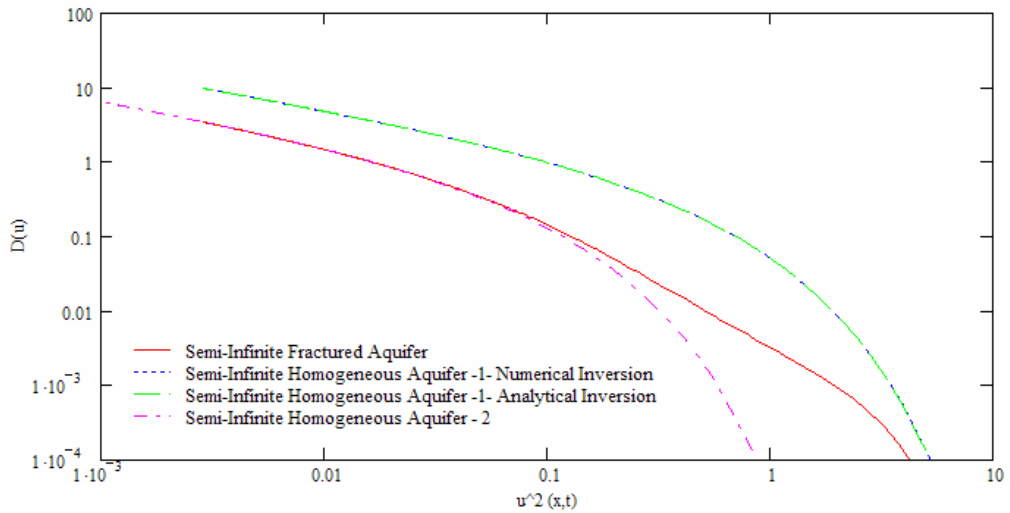
Figure 5.1: $D(u)$ vs. $u^2(x,t)$ on a log-log scale

As expected the graphs of the results for the numerical solution and the exact solution for homogeneous case are exactly the same showing that the results of the numerical inversion gives the same results as the exact solution.

The graphic for the semi-infinite fractured case is asymptotic to the homogeneous case for smaller $u(x,t)$ values, and as $u(x,t)$ increases the head starts to decrease faster than the homogeneous case. Physically this can be explained by the fact that in the fractured aquifer case the storage in the blocks moves to the fractured hence the drawdown is not as much as the homogeneous case.
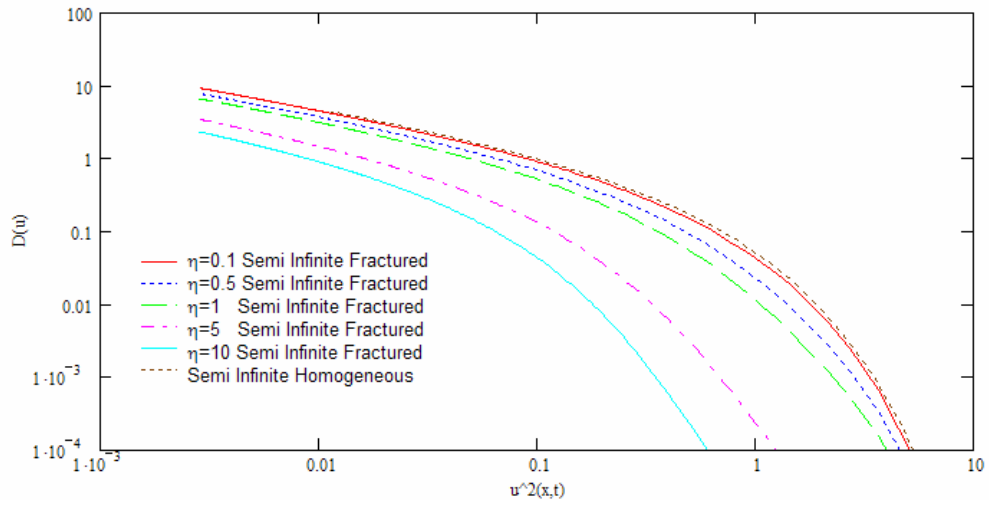
Figure 5.2: $D(u)$ vs. $u^2(x,t)$ on a log-log scale for constant δ =5 and various η values – Semi-infinite Fractured Aquifer
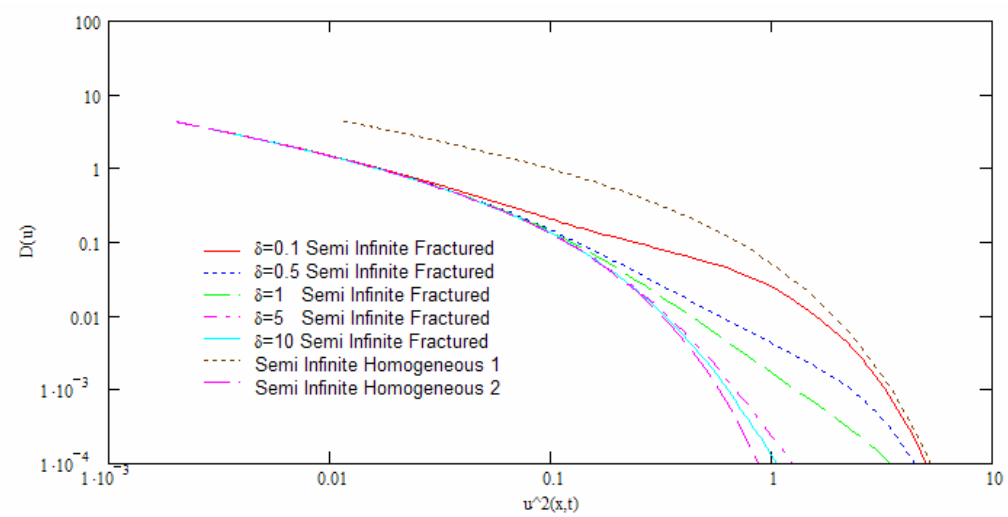
Figure 5.3: $D(u)$ vs. $u^2(x,t)$ on a log-log scale for constant η =5 and various δ values - Semi-infinite Fractured Aquifer

5.3 Comparison of Results – Finite Fractured Aquifer

As demonstrated in the previous example below graphics are drawn to make the same comparison against the semi-infinite fractured aquifer problem.

Below constant are used to draw the graphics in this chapter:

$$v = 0.135 \qquad Q_d = 0.065 \qquad S_1 = 2.10^{-6} \qquad T_1 = 2.10^{-7} \, m^2 / \sec \qquad \eta = 5$$

$$\delta = 0.625 \qquad L = 100m \qquad h_0 = 20m \ \text{where} \ v = \frac{T_1}{S_1}$$
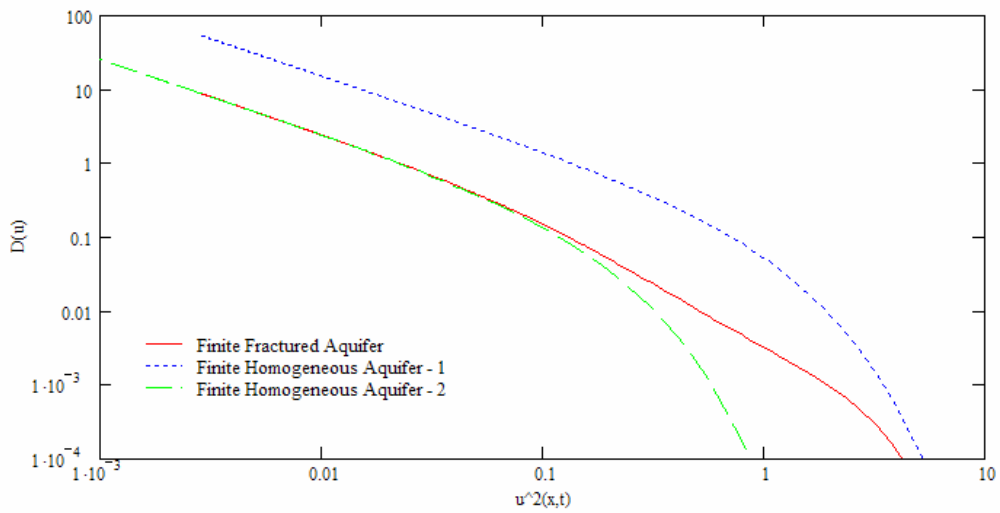
Figure 5.4: $D(u)$ vs. $u^2(x,t)$ on a log-log scale
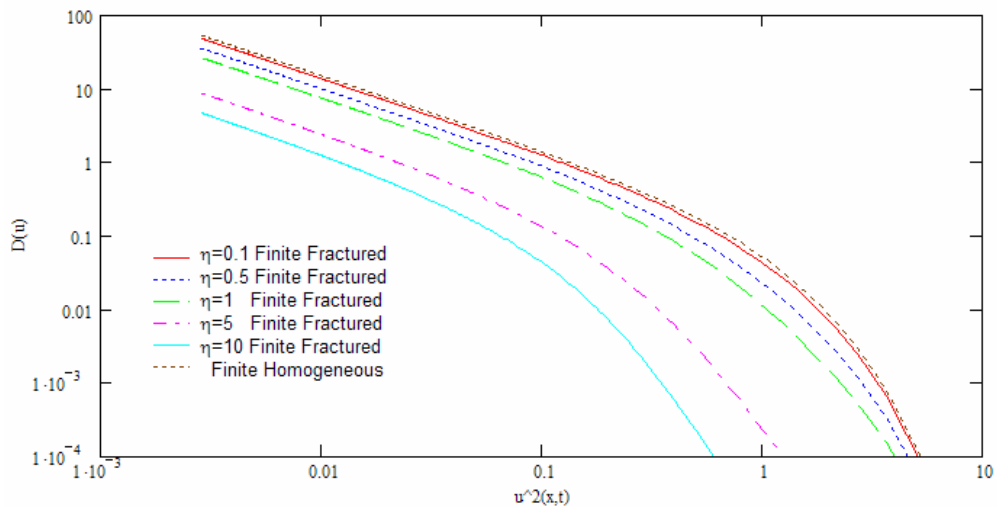
Figure 5.5: $D(u)$ vs. $u^2(x,t)$ on a log-log scale for constant $\delta = 5$ and various η values – Finite Fractured Aquifer
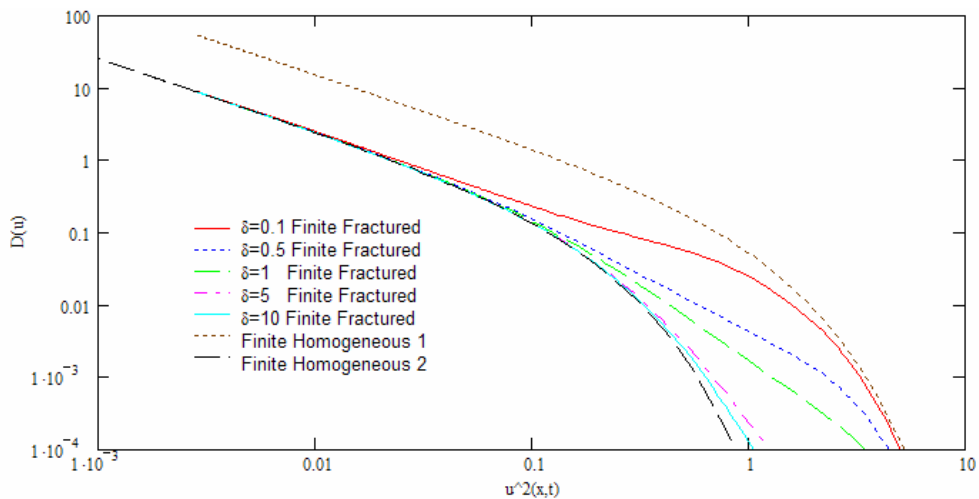
Figure 5.6: $D(u)$ vs. $u^2(x,t)$ on a log-log scale for constant $\eta = 5$ and various δ values – Finite Fractured Aquifer

Unfortunately no reliable field data is available to compare results to the field values. As seen from Figure 5.4 the graph of the finite-fractured case is becoming asymptotic to the homogeneous case for smaller $u(x,t)$ values. And as D(u) increases the head starts to decrease faster than the homogeneous case. Comparing Figure 5.1 & Figure 5.4 shows that, in the finite fractured case after some point –the

54

effect of boundary starts to appear- D(u) begins to increase faster than the semi-infinite case as $u(x,t)$ decreases. This can be seen easier in the below graph 5.7.
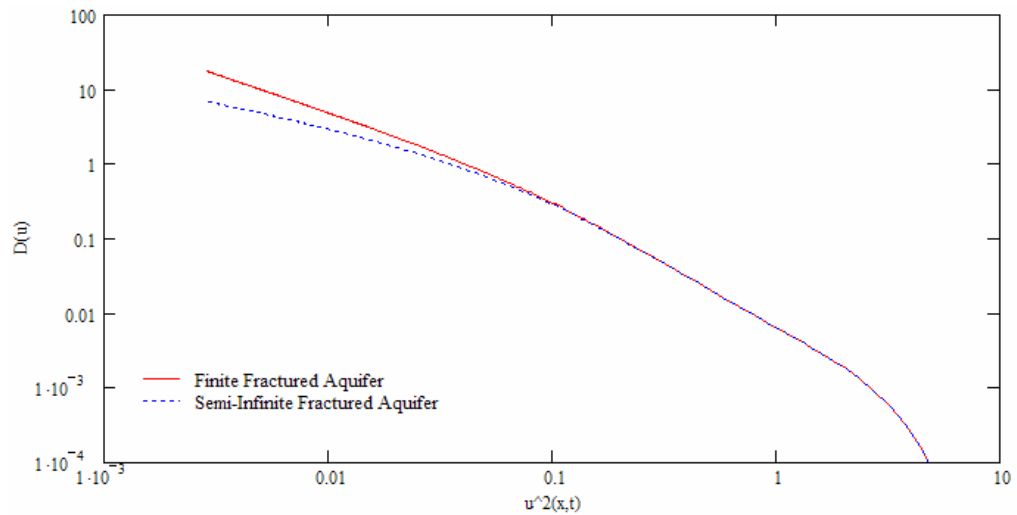
Figure 5.7: $D(u)$ vs. $u^2(x,t)$ on a log-log scale for semi-infinite and finite fractured aquifer cases.
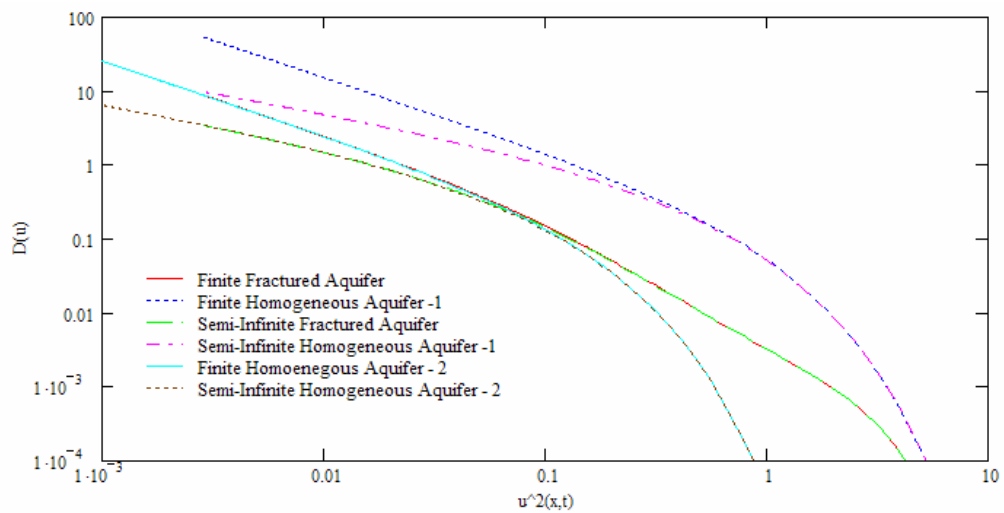
Figure 5.8: $D(u)$ is plotted against $u^2(x,t)$ on a log-log scale for semi-infinite and finite fractured and homogeneous aquifer cases.

The results of this chapter are summarised above in Figure 5.8. As can be seen from this graph, the homogeneous case graphs and the fractured case graphs become asymptotic as $u^2(x,t)$ decreases. Whereas finite and semi-infinite case graphs become asymptotic as $u^2(x,t)$ increases.

CHAPTER 6

SUMMARY AND CONCLUSIONS

Fluid flow in fractured media is gaining increasing importance especially in petroleum geology, mining engineering, and karstic terrain hydrogeology. Analytical methods are commonly used to analyze water level changes occur in response to groundwater pumpage. These methods permit determination of aquifer properties and prediction of aquifer response which are needed in the evaluation of the groundwater resources of a given region. Although many analytical solutions are available to groundwater hydrologists, not all of them are readily evaluated.

In this study an attempt is made to demonstrate the advantage of working in Laplace plane. The unsteady flow in the aquifer resulting from a constant discharge pumped from the stream was investigated. Both a finite and semi-infinite aquifer is considered. The governing differential equations of the flow, which are based on the double porosity medium conceptual model with pseudo-steady state transfer of water between the fractures and blocks, were solved analytically in the Laplace plane first, and inverted to the real plane by using a numerical inversion technique: Stehfest algorithm. The solutions are presented for a set of aquifer parameters in terms of piezometric head vs. time and piezometric head vs. distance.

Ferris' equations are used to make comparisons between the homogeneous and fractured cases as well as between semi-infinite and finite cases.

According to the graphs plotted, it is seen that as time goes to zero or infinity; the flow behaviour is same in both fractured and homogeneous cases, as they approach each other asymptotically. The reason behind this is: The discharge taken from the stream is a disturbance to the system, the flow from blocks to the fractures start to occur after a certain period time. In the first instance there will only be flow in fractures without the flow from blocks to the fractures. So during this short period of time the blocks can not respond to the disturbance. This makes the behaviour similar to that of the homogeneous case – where there are no blocks-. On the right hand side of the Figure 5.3 and 5.6 the graph for the homogeneous case shows this limit case, where the fractured flow graphics approach to this graph for short time. There is also another limit defined at the left hand side of the Figures 5.3 and 5.6. This is for a hypothetical homogeneous aquifer which has the storage capacity equal to that of the blocks plus the fractures, whereas having the transmissivity coefficient the same as the fractures. The fractured case graphs approach to this limit case as time goes to infinity. The reason behind is as the discharge is taken from the stream for long periods the system finds a second form of equilibrium where the blocks and fractures act as one member, both of them having the same pressure. Since there is no pressure difference between the fractures and blocks there can't be any flow between them which is the same behaviour that can be observed in an homogeneous aquifer.

It is also observed from the figures that, the fractured aquifers have always less drawdown then the homogeneous aquifers. The reason behind is there is flow from the blocks to the fractures which keeps the piezometric head level in the fractures higher then the

piezometric head in the homogeneous aquifer. As explained in the previous paragraph this is not true for very short and very long times.

From Figure 5.6 it can also be seen that the flow behaviour in semi-infinite and finite fractured aquifers are exactly the same for quite some time. A critical time can be observed from the graph at which the effect of the boundary in the finite fractured aquifer starts to appear and these two graphs starts to differ from each other. The finite fractured aquifer has always more drawdown then the semi-infinite fractured aquifer after this critical time. Because, in the semi-infinite fractured case there is always flow coming from the blocks to the fractures, since the length of the aquifer in infinite. Whereas in the finite aquifer there is an impervious boundary so there is limited amount of water which can feed the flow in the fractures.

REFERENCES

Barenblatt, G. I.,Zheltov, I.P.& Kochina, I.N. (1960). Basic concepts in the theory of seepage of homogeneous liquids in fractured rocks (strata) J. Appl. Mat. And Mech. 24(5), 1286-1303

Bear, J., (1979). Hydraulics of groundwater: New York, McGraw-Hill Book Company.

Bear, J., Tsang, C.F. & de Marsily, G. (1993). Flow and contamination transport in fractured rock. Academic Press, San Diego, USA.

Boulton, N.S. and Streltsova, T.D., (1977), Unsteady Flow to a Pumped Well in a Fissured Water-Bearing Formation, Journal of Hydrology, v.35, pp 257-269.

Ferris, J.G., Knowles, D.B., Brown, R.H., and Stallman, R.W., (1962), Theory of Aquifer Tests: U.S. Geol. Survey Water-Supply Paper 1536-E, p. 69-174

Hall, F.R., and Moench, A.F. (1972). Application of the convolution equation to stream-aquifer relationships, Water Resources Research, Vol 8, No 2.

Huyakorn, P.S.&Pinder, G.F. (1983) Computational Methods in Subsurface Flow. Academic Press, New York.

Hsieh, P., (2002). GES236 – Hydraulic and tracer tests or groundwater resource evaluation – Lecture Notes. Stanford University, Stanford.

Jenkins, D. N. and Prentice J. K., (1982). Theory for Aquifer Test Analysis in Fractured Rocks Under Linear (Nonradial) Flow Conditions. Ground Water, January/February 1982, 12-21.

Kazemi, H. (1969) Pressure transient analysis of naturally fractured reservoirs with uniform fracture distribution. Soc. Pet. Engng J. 9, 451-462.

Kazemi, H., Seth, M.S. & Thomas, G.W. (1969) The interpretation of interferance tests in naturally fractured reservoirs with uniform fracture distribution. Soc. Pet. Engng J. 9, 463-472.

Lohman, S. W., (1988). Geological Survey Professional Paper 708. Groundwater Hydraulics. US Government Printing Office, Washington, 1972, 40-41.

Moench, A.F. (1984), Double porosity models for a fractured groundwater reservoir with fracture skin. Wat. Resor. Res. 20(7), 831-846.

Moench, A. F. and Barlow, P. M., (2000). Aquifer response to stream-stage and recharge variations. Journal of Hydrology, 230 (2000), 192-210.

Moench, Allen, and Ogata, Akio, (1984), Analysis of constant discharge wells by numerical inversion of Laplace transform solutions, in Rosenshein, J.S., and Bennett, G.D., eds., Groundwater Hydraulics: Water Resources Monograph 9, American Geophysical Union, Washington D.C., p. 146-170.

Motz, L. H. (2002). <u>Leaky One-Dimensional Flow with Storage and Skin Effect in Finite-Width Sink</u>. Journal of Irrigation and Drainage Engineering, September/October(2002), 298-304.

Önder, H., (1994). <u>Determination of aquifer parameters of finite confined aquifers from constant drawdown non-steady type-curves.</u> Hydrol. Sci. J.39(3), 269-280.

Önder, H., (1997). <u>Analysis of one-dimensional groundwater flow in a nonuniform aquifer</u>. Journal of Hydraulic Engineering, August 1997, 732-736.

Önder, H., (2002). <u>Predicting groundwater flow behaviour in non-uniform aquifers in contact with a stream: an extension to ditch drainage</u>. Current Problems of Hydrogeology in Urban Areas. Urban Agglomerates and Industrial Centers, 2002, 407-423.

Önder, H. (1998). <u>One-dimensional transient flow in a finite fractured aquifer.</u> Hydrological Sciences-Journal des Sciences Hydrologiques, 43(2) April 1998, 243-260.

Pinder, G. F, Breedhoeft, J.D. & Cooper, H. H. (1969) <u>Determination of aquifer diffusivity from aquifer response to fluctuations in river stage</u>. Wat. Resour. Res. 5(4), 850-855.

Rorabaugh, M.I. (1960) <u>Use of water levels in estimating aquifer constants in a finite aquifer</u>. In: Commision of Subterranean Waters, 314-323. IAHS Publ. No. 52

Rorabaugh, M.I. (1964) <u>Estimating changes in bankstorage and gorundwater contribution to stream flow.</u>In: Symposium of Surface Waters, 432-441. IAHS Publ. N :63.

Sen, Z., (1986). <u>Aquifer Test Analysis in Fractured Rocks with Linear Flow Pattern</u>. Ground Water, Vol24 No.1, January-February 1986, 72-78.

Stehfest, H., (1970) <u>Numerical Inversion of Laplace transforms</u>, Commun. ACM, 13(1), 47-49.

Streltsova, T.D. (1976). <u>Hydrodynamics of groundwater flow in a fractured formation.</u> Wat. Resour. Res. 12(3), 405-414.

Streltsova, T.D. (1988). <u>Well testing in heterogeneous formations,</u> John Wiley, New York, USA.

Tomasko, D., (?).<u>Optimally Orienting a Parallel-Strip Aquifer Using Multiwell Test Data</u>. Journal of the Institute of Civil Engineers, Vol. 15, 81-93.

Venetis, C., (1970) <u>Finite aquifers: characteristic responses and applications</u>. J. Hydrol. 22, 53-62.

Warren, J.E. & Root, P.J. (1963) <u>The behaviour of naturally fractured reservoirs.</u> Soc. Pet. Engng J. 3, 245-255.

APPENDIX A

SUBROUTINE USED TO SOLVE THE STEHFEST ALGORITHM NUMERICALLY

Function calculating the results of the Stehfest algorithm computations

for predefined N,x,t :

$$V(i, N) := (-1)^{\left(\frac{N}{2}+i\right)} \cdot \sum_{k = \text{trunc}\left[\frac{(i+1)}{2}\right]}^{\min\left(i, \frac{N}{2}\right)} \frac{k^{\left(\frac{N}{2}\right)} \cdot (2\,k)!}{\left(\frac{N}{2} - k\right)! \cdot (k)! \cdot (k - 1)! \cdot (i - k)! \cdot (2\,k - i)!}$$

$u(x, p)$ is the analytical solution which found by using Laplace transform

method

$$\text{Main}(p, x, t) := \begin{vmatrix} \text{for } i \in 1.. N \\ \begin{vmatrix} R_{i, 1} \leftarrow i \\ R_{i, 2} \leftarrow V(i, N) \\ p2 \leftarrow i \cdot p \\ R_{i, 3} \leftarrow u(x, p2) \\ R_{i, 4} \leftarrow R_{i, 2} \cdot R_{i, 3} \end{vmatrix} \\ \text{Sum} \leftarrow \sum_{i = 1}^{N} R_{i, 4} \\ \begin{pmatrix} R \\ \text{Sum} \end{pmatrix} \end{vmatrix}$$

$$\text{Table2}(p, x, t) := \begin{vmatrix} X_{1, 1} \leftarrow \text{"i"} \\ X_{1, 2} \leftarrow \text{"Vi"} \\ X_{1, 3} \leftarrow \text{"u(x,p)"} \\ X_{1, 4} \leftarrow \text{"(Vi) * u(x,p)"} \\ \text{stack}\left(X, \text{Main}(p, x, t)_1\right) \end{vmatrix}$$

$$\text{Table} := \text{Table2}\left(\frac{\ln(2)}{4}, 2, 4\right)$$

A.1: Sample Results of Stehfest Algorithm computations for particular t,x and N values. (t=4, x=2, v =1, N=10)

$$
\text{Table} =
\begin{pmatrix}
\text{"i"} & \text{"Vi"} & \text{"u(x,p)"} & \text{"(Vi) * u(x,p)"} \\
1 & 0.083333 & 2.509924 & 0.20916 \\
2 & -32.083333 & 0.888918 & -28.519463 \\
3 & 1.279 \times 10^3 & 0.45483 & 581.727374 \\
4 & -1.562367 \times 10^4 & 0.272915 & -4.263927 \times 10^3 \\
5 & 8.424417 \times 10^4 & 0.179375 & 1.511126 \times 10^4 \\
6 & -2.369575 \times 10^5 & 0.125145 & -2.965393 \times 10^4 \\
7 & 3.759117 \times 10^5 & 0.091097 & 3.424426 \times 10^4 \\
8 & -3.400717 \times 10^5 & 0.068464 & -2.32825 \times 10^4 \\
9 & 1.640625 \times 10^5 & 0.052756 & 8.655252 \times 10^3 \\
10 & -3.28125 \times 10^4 & 0.04148 & -1.361059 \times 10^3
\end{pmatrix}
$$

For a particular point in time the results are found by using below functions;

$$\text{Result} := \text{Main}\left(\frac{\ln(2)}{4}, 2, 4\right)_2$$

Function computing the Laplace Domain Solution

$$\text{Result2} := \text{Result} \cdot \left(\frac{\ln(2)}{4}\right)$$

Function inverting the solution in Laplace Domain to real domain

APPENDIX B

SUBROUTINES USED TO DRAW COMPARISON GRAPHS

B.1: The subroutine written to plot dimensionless drawdown vs. dimensionless time for a constant dimensionless distance y. Where the drawdown is calculated using the numerical inversion method.

$$z_{stehfest}(y) := \begin{vmatrix} \theta_1 \leftarrow 2 \\ \text{for } k \in 2..50 \\ \quad \begin{vmatrix} z_{k-1} \leftarrow \text{Main}\left(\dfrac{\ln(2)}{\theta_{k-1}}, y, \theta_{k-1}\right) 2 \cdot \dfrac{\ln(2)}{\theta_{k-1}} \\ \theta_k \leftarrow \theta_{k-1} + k \cdot 0.14 \end{vmatrix} \\ \begin{pmatrix} z \\ \theta \end{pmatrix} \end{vmatrix}$$

B.2: The subroutine written to plot dimensionless drawdown vs. dimensionless distance for a constant dimensionless time. Where the drawdown is calculated using the numerical inversion method.

$$z2_{stehfest}(\theta) := \begin{vmatrix} y_1 \leftarrow 0.1 \\ \text{for } k \in 2..50 \\ \quad \begin{vmatrix} z_{k-1} \leftarrow \text{Main}\left(\dfrac{\ln(2)}{\theta}, y_{k-1}, \theta\right) 2 \cdot \dfrac{\ln(2)}{\theta} \\ y_k \leftarrow y_{k-1} + k \cdot 0.1 \end{vmatrix} \\ \begin{pmatrix} z \\ y \end{pmatrix} \end{vmatrix}$$

APPENDIX C

SUBROUTINES USED FOR COMPARISONS WITH FERRIS' EQUATIONS

C1: Subroutine to draw $D(z,y)$ vs. $u^2(y,\theta)$ for the finite fractured aquifer with constant discharge problem. (Numerical Solution)

$$\text{Solve1} := \begin{vmatrix} y \leftarrow 3 \\ \theta \leftarrow 0.05 \\ \text{for } k \in 1..400 \\ \quad \begin{vmatrix} z_k \leftarrow \text{Main}\left(\dfrac{\ln(2)}{\theta}, y, \theta\right) 2\cdot\left(\dfrac{\ln(2)}{\theta}\right) \\ u_k \leftarrow \dfrac{y}{2\sqrt{\theta}} \\ D_k \leftarrow \dfrac{z_k}{Q_d \cdot y} \\ \theta \leftarrow \theta + 0.01k \end{vmatrix} \\ \begin{pmatrix} z \\ u \\ D \end{pmatrix} \end{vmatrix}$$

C2: Subroutine to draw $D(u)$ vs. $u^2(x,t)$ for finite homogeneous aquifer with constant discharge problem. (Numerical Solution)

$$Solve2 := \begin{vmatrix} x \leftarrow 60 \\ t \leftarrow 50 \\ \text{for } k \in 1..400 \\ \quad \begin{vmatrix} z_k \leftarrow Main4\left(\dfrac{\ln(2)}{t}, x, t\right) 2 \cdot \left(\dfrac{\ln(2)}{t}\right) \\ u_k \leftarrow x \cdot \sqrt{\dfrac{S}{4 \cdot T \cdot t}} \\ D_k \leftarrow \dfrac{2 \cdot z_k}{Q_d \cdot x} \\ t \leftarrow t + 29.58 k \end{vmatrix} \\ \begin{pmatrix} z \\ u \\ D \end{pmatrix} \end{vmatrix}$$

C3: Subroutine to draw $D(z,y)$ vs. $u^2(y,\theta)$ for semi-infinite fractured aquifer with constant discharge problem. (Numerical Solution)

$$Solve3 := \begin{vmatrix} y \leftarrow 3 \\ \theta \leftarrow 0.05 \\ \text{for } k \in 1..400 \\ \quad \begin{vmatrix} z_k \leftarrow Main2\left(\dfrac{\ln(2)}{\theta}, y, \theta\right) 2 \cdot \left(\dfrac{\ln(2)}{\theta}\right) \\ u_k \leftarrow \dfrac{y}{2\sqrt{\theta}} \\ D_k \leftarrow \dfrac{z_k}{Q_d \cdot y} \\ \theta \leftarrow \theta + 0.01 k \end{vmatrix} \\ \begin{pmatrix} z \\ u \\ D \end{pmatrix} \end{vmatrix}$$

C4: Subroutine to draw $D(u)$ vs. $u^2(x,t)$ for semi-infinite homogeneous aquifer with constant discharge problem. (Exact Solution)

$$
\text{Solve4} := \begin{vmatrix} x \leftarrow 60 \\ t \leftarrow 50 \\ \text{for } k \in 1..400 \\ \quad \begin{vmatrix} u_k \leftarrow x \cdot \sqrt{\dfrac{S}{4 \cdot T \cdot t}} \\[2ex] D_k \leftarrow \dfrac{e^{-(u_k)^2}}{u_k \cdot \sqrt{\pi}} - 1 + \text{erf}(u_k) \\[2ex] z_k \leftarrow Q_d \cdot x \cdot D_k \\ t \leftarrow t + 29.58\,k \end{vmatrix} \\ \begin{pmatrix} z \\ u \\ D \end{pmatrix} \end{vmatrix}
$$

C5: Subroutine to draw $D(u)$ vs. $u^2(x,t)$ for semi-infinite homogeneous aquifer with constant discharge problem. (Numerical Solution)

$$
\text{Solve5} := \begin{vmatrix} x \leftarrow 60 \\ t \leftarrow 50 \\ \text{for } k \in 1..400 \\ \quad \begin{vmatrix} z_k \leftarrow \text{Main3}\left(\dfrac{\ln(2)}{t}, x, t\right) 2 \cdot \left(\dfrac{\ln(2)}{t}\right) \\[2ex] u_k \leftarrow x \cdot \sqrt{\dfrac{S}{4 \cdot T \cdot t}} \\[2ex] D_k \leftarrow \dfrac{2 \cdot z_k}{Q_d \cdot x} \\[2ex] t \leftarrow t + 29.58\,k \end{vmatrix} \\ \begin{pmatrix} z \\ u \\ D \end{pmatrix} \end{vmatrix}
$$

C6: Subroutine to draw $D(u)$ vs. $u^2(x,t)$ for finite homogeneous aquifer with constant discharge. Max. storage limit case (Numerical Solution)

$$
\text{Solve6} := \begin{vmatrix}
x \leftarrow 60 \\
t \leftarrow 50 \\
\text{for } k \in 1..400 \\
\quad \begin{vmatrix}
z_k \leftarrow \text{Main4}\left(\dfrac{\ln(2)}{t}, x, t\right) 2 \cdot \left(\dfrac{\ln(2)}{t}\right) \\[2mm]
u1_k \leftarrow \dfrac{x}{\sqrt{1+\eta}} \cdot \sqrt{\dfrac{S}{4 \cdot T \cdot t}} \\[2mm]
u_k \leftarrow x \cdot \sqrt{\dfrac{S}{4 \cdot T \cdot t}} \\[2mm]
D_k \leftarrow \dfrac{2 \cdot z_k}{Q_d \cdot x} \\[2mm]
t \leftarrow t + 29.58 k
\end{vmatrix} \\[2mm]
\begin{pmatrix} z \\ u1 \\ D \end{pmatrix}
\end{vmatrix}
$$

C7: Subroutine to draw $D(u)$ vs. $u^2(x,t)$ for semi-infinite homogeneous aquifer with constant discharge. Max. storage limit case (Numerical Solution)

$$Solve7 := \begin{vmatrix} x \leftarrow 60 \\ t \leftarrow 50 \\ \text{for } k \in 1..400 \\ \quad \begin{vmatrix} z_k \leftarrow Main3\left(\dfrac{\ln(2)}{t}, x, t\right) 2 \cdot \left(\dfrac{\ln(2)}{t}\right) \\ u1_k \leftarrow \dfrac{x}{\sqrt{1+\eta}} \cdot \sqrt{\dfrac{S}{4 \cdot T \cdot t}} \\ u_k \leftarrow x \cdot \sqrt{\dfrac{S}{4 \cdot T \cdot t}} \\ D_k \leftarrow \dfrac{2 \cdot z_k}{Q_d \cdot x} \\ t \leftarrow t + 29.58 k \end{vmatrix} \\ \begin{pmatrix} z \\ u1 \\ D \end{pmatrix} \end{vmatrix}$$